Elevated glucose levels promote contractile and cytoskeletal gene expression in vascular smooth muscle via Rho/protein kinase C and actin polymerization.

Hien Tran, Thi; Turczynska, Karolina; Dahan, Diana; Ekman, Mari; Grossi, Mario; Sjögren, Johan; Nilsson, Johan; Braun, Thomas; Boettger, Thomas; Garcia Vaz, Eliana; Stenkula, Karin; Swärd, Karl; Gomez, Maria; Albinsson, Sebastian

Published in:
Journal of Biological Chemistry

DOI:
10.1074/jbc.M115.654384

Published: 2016-01-01

Document Version
Peer reviewed version (aka post-print)

Elevated glucose levels promote contractile and cytoskeletal gene expression in vascular smooth muscle via Rho/protein kinase C and actin polymerization

Tran Thi Hien[1], Karolina M.Turczyńska[1], Diana Dahan[1], Mari Ekman[1], Mario Grossi[1], Johan Sjögren[2], Johan Nilsson[2], Thomas Braun[3], Thomas Boettger[3], Eliana Garcia-Vaz[4], Karin Stenkula[1], Karl Swärd[1], Maria F. Gomez[4] and Sebastian Albinsson[1]

[1] From the Department of Experimental Medical Sciences, Lund University, Sweden
[2] Department of Clinical Sciences, Lund University, Sweden
[3]Max Planck Institute for Heart and Lung Research, Bad Nauheim, Germany
[4] Department of Clinical Sciences in Malmö, Lund University, Sweden

[*]Running title: *Glucose-induced gene expression in smooth muscle*

To whom correspondence should be addressed: Dr. Sebastian Albinsson
Department of Experimental Medical Science, Lund University, BMC D12, SE-221 84 Lund, Sweden
Tel: +46-46-2227765, Fax: +46-46-2113417, E-mail: sebastian.albinsson@med.lu.se

Keywords: Glucose, vascular smooth muscle cells, diabetes, microRNA, cell differentiation, Rho, actin polymerization

ABSTRACT

Both type 1 and type 2 diabetes are associated with increased risk of cardiovascular disease. This is in part attributed to the effects of hyperglycemia on vascular endothelial and smooth muscle cells but the underlying mechanisms are not fully understood. In diabetic animal models, hyperglycemia results in hyper-contractility of vascular smooth muscle possibly due to increased activation of Rho-kinase. The aim of the present study was to investigate the regulation of contractile smooth muscle markers by glucose and to determine the signaling pathways that are activated by hyperglycemia in smooth muscle cells.

Microarray, qPCR and western blot analyses revealed that both mRNA and protein expression of contractile smooth muscle markers was increased in isolated smooth muscle cells cultured under high compared to low glucose conditions. This effect was also observed in hyperglycemic Akita mice and in diabetic patients. Elevated glucose activated the protein kinase C and Rho/Rho-kinase signaling pathways and stimulated actin polymerization. Glucose-induced expression of contractile smooth muscle markers in cultured cells could be partially or completely repressed by inhibitors of advanced glycation end products, L-type calcium channels, protein kinase C, Rho-kinase, actin polymerization and myocardin related transcription factors. Furthermore, genetic ablation of the miR-143/145 cluster prevented the effects of glucose on smooth muscle marker expression.

In conclusion, these data demonstrate a possible link between hyperglycemia and vascular disease states associated with smooth muscle contractility.

Diabetes confers a two- to four-fold excess risk for a wide range of cardiovascular diseases, including macrovascular complications leading to coronary heart disease and ischemic stroke, as well as microvascular diseases such as nephropathy and retinopathy (1,2). Based on current trends, the rising incidence of diabetes (expected to reach 333 million people worldwide by 2025), will undoubtedly equate to increased cardiovascular mortality. Chronic hyperglycemia has long been recognized as an independent risk factor for cardiovascular disease (3,4). Importantly, the progressive relationship between glucose levels and cardiovascular risk extends below the threshold for diabetes diagnosis (fasting plasma glucose ≥7.0mmol/l or 2–h plasma glucose

≥11.1mmol/l (2,3)) and more recently, even transient hyper- or hypoglycemia have emerged as important determinants of cardiovascular disease (5). Despite the vast clinical and epidemiological experience linking blood glucose and poor glucose control to the development and progression of cardiovascular disease, the underlying molecular mechanisms leading to vascular dysfunction and disease are poorly understood (6).

It has been well established that hyperglycemia results in vascular hyper-reactivity in diabetic patients (7) and animal models (8-10) Part of this effect may be attributed to a decrease in nitric oxide (NO) bioavailability, as well as a reduced response of vascular smooth muscle cells (VSMCs) to NO (11). However, hyperglycemia can also cause an endothelium-independent hypercontractility of smooth muscle cells (8,10,12). The underlying mechanism behind this effect is in part due to activation of the PKC/Rho/Rho-kinase pathway by glucose, which results in calcium sensitization by inhibiting myosin light chain phosphatase (12-15). The activation of PKC and Rho in smooth muscle by hyperglycemia is thought to be dependent on the formation of advanced glycation end products (AGE) (16,17).

In addition to calcium sensitization, activation of the Rho/Rho-kinase pathway in VSMCs promotes actin polymerization, an effect that plays a major role in the regulation of smooth muscle gene expression and activates myocardin related transcription factors (MRTFs aka. MKL1/2), co-factors to serum response factor (SRF) (18,19). Monomeric actin sequesters MRTFs and inhibits their activity by preventing interaction with SRF. When actin is polymerized, MRTFs are released and can associate with SRF in the nucleus. SRF binds to genetic elements referred to as CArG boxes (CC-A/T_6-GG) and this binding is antagonized by the transcription factor Krüppel-like factor 4 (20). We have previously demonstrated that actin polymerization is crucial for stretch-induced contractile differentiation in vascular smooth muscle (21-24). Further, we reported that important regulators of smooth muscle differentiation such as the small non-coding microRNA miR-145 promotes actin polymerization and that this effect is required for the regulation of contractile smooth muscle genes (25-27). However, the impact of actin polymerization on smooth muscle gene expression in the context of diabetic vascular disease has not yet been explored.

Herein, we aimed to determine the effects of extracellular glucose on vascular smooth muscle contractile differentiation. This was investigated using isolated smooth muscle cells in culture, arteries from hyperglycemic Akita mice and mammary arteries from diabetic patients.

EXPERIMENTAL PROCEDURES

Animals - MicroRNA-143/145 knockout (KO) mice were generated at the Max-Plank-Institute for Heart and Lung research as described (28). Wild type (WT) littermates were used as controls.

Akita type 1 diabetic mice (C57BL/6-*Ins2*$^{C96Y/+}$/J) were obtained from the Jackson laboratory and bred at Lund University. Mice were euthanized by exsanguination through cardiac puncture under deep anesthesia. Mesenteric arteries from adult 12 week old male heterozygous Akita and littermate wild-type non-diabetic control mice were placed in RNAlater (cat#76104; Qiagen) and dissected free from fat and surrounding tissue.

All experiments were approved by the Malmö/Lund animal ethics committee. This investigation conforms to Directive 2010/63/EU of the European Parliament.

Human samples - Left internal mammary arteries (LIMA) from patients undergoing bypass surgery were obtained in collaboration with surgeons at Skåne University Hospital in Lund. The vessels were immediately placed in ice cold HEPES-buffer, dissected free from fat and surrounding tissue and snap frozen in liquid nitrogen. All participants gave their informed consent. The study protocols conformed to the Declaration of Helsinki and were approved by local Human Ethics Committee.

Cell culture - Vascular smooth muscle cells were isolated from miR-143/145 KO and WT mouse aorta by enzymatic digestion and maintained in culture as described (27). Mouse aortic smooth muscle cells from passage 3 were cultured in DMEM (Gibco #11966-025) supplemented with low glucose (1.7 mM glucose), normal glucose (5.5 mM glucose), high glucose (25 mM glucose) or low glucose plus mannitol

(1.7 mM glucose + 23.3 mM mannitol) for 1-6 weeks. The medium was routinely exchanged every 48h. All media were supplemented with 10% fetal bovine serum (Biochrom #S0115) and 50U/50µg/ml penicillin/streptomycin (Biochrom, A2212). Cells were passaged approximately every 10 days during glucose treatment. Cells were treated with Latrunculin B 250nM (Calbiochem, cat no. 76343-94-7), Y-27632 10 µM (Tocris #1254), CCG-1423 10 µM (Calbiochem #555558), GFX 10 µM (Sigma Aldrich #B6292), verapamil 1 µM (Sigma Aldrich #V4629) aminoguanidine hydrochloride (AMG) 100 µM (Sigma Aldrich #A7009) or 0,1% DMSO as a vehicle control for the last 24 hours of a one week incubation. The MTT cell viability assay was used to exclude any cytotoxic effects of the inhibitors.

siRNA experiments were performed using Silencer® Select Pre-Designed siRNA (#: 4390771, Thermo Scentific). Cells were transfected with 20 nM MKL1 siRNA (ID: s73019), 20 nM MKL2 siRNA (ID: s109074), 20 nM ROCK1 siRNA (ID: s104595), 20 nM ROCK2 siRNA (ID: s73020) or 20 nM control siRNA using Oligofectamin transfection reagent (Invitrogen) for 96 hr. In some experiments, cells were transfected with 10nM MKL1+10 nM MKL2 siRNA or 10nM ROCK1+10 nM ROCK2 siRNA. Each siRNAs caused approximately 50% reduction in the expression of its respective target gene.

Quantitative real-time PCR (qRT-PCR) - Total RNA was isolated using miRNeasy mini kit (Qiagen, #217004) as described previously (29). Purity and concentration were determined with an ND-1000 spectrophotometer (Nanodrop Technologies Inc., Wilmington, DE, USA). The expression of mRNA was analyzed by real-time qPCR (StepOnePlus qPCR cycler, Applied Biosystems) using QuantiFast SYBR Green RT-PCR Kit Qiagen, #204156) and QuantiTect primer assays: Mouse - Mm_Kcnmb1, QT00101500; Mm_Tagln, QT00165179; Mm_Cnn1, QT00105420, Mm_GADPH, QT01658692; Mm_Dmd, QT00161336; Mm_Des, QT00102333; Mm_Dcn, QT00131068, Mm_Ptgs2 (COX-2), QT00165347; Mm_Tnf, QT00165347; Mm_Mglap, QT00145775; Mm_Spp1, QT02524536. Primer sequences are proprietary of Qiagen.

Microarray analysis - RNA was extracted using the RNeasy Mini Kit (Qiagen #74106). Purity and concentration were determined with an ND-1000 spectrophotometer (Nanodrop Technologies Inc., Wilmington, DE, USA). After passing quality control by Agilent Bioanalyzer, total RNA was analyzed by Affymetrix GeneChip® Mouse Gene 2.0 ST Array at the Swegene Center for Integrative Biology at Lund University (SCIBLU). The microarray data is accessible via the Gene Expression Omnibus (accession number GSE66280, scheduled release on 1 July 2015).

Transcription factor binding site analysis was made using the online tool oPOSSUM (http://opossum.cisreg.ca/). q=0 was used as cut-off and default search parameters were chosen throughout.

Protein extraction and Western Blotting - Cells grown on 6-well plates were washed twice with ice-cold PBS and lysed on ice directly in the wells with 75 µl of 1x Laemmli sample buffer (60 mM Tris-HCl, pH 6.8, 2% SDS, 10% glycerol). Frozen tissue was pulverized using liquid nitrogen as described previously (30). Proteins were detected using commercially available primary antibodies: α-actin (1:2000, Sigma Aldrich, #A5528), calponin (1:1000, Abcam, #ab46784), SM22α (1:5000, Abcam, #ab14106), phospho-ERM (Ezrin (Thr567)/Radixin (Thr564)/Moesin (Thr558)) (1:1000, Cell Signaling, #3141S), total-ERM (Cell Signaling, #3142S), total and phospho-cofilin-2 (Ser3) (1:500, Merck Millipore, #07-300 and 07-326), phospho-LIMK1 (Thr508) (1:1000, Cell Signaling, #3841S), LIMK-1 (1:1000, Cell Signaling, #3842s), phospho-MYPT (Thr696) (1:1000, Cell Signaling, #5163S), MYPT (1:1000, Cell Signaling, #2634s) HSP90 (1:1000, BD Transduction Laboratories, #610418), β-actin (1:2000, Sigma Aldrich, #A5441), Phospho-(Ser) PKC Substrate (1:1000, Cell Signaling, #2261S), AMPKα (1:1000, Cell Signaling, #2603), T172-phospho-AMPKα (1:1000, Cell Signaling, #2535), S79-phospho-ACC (1:1000, Cell Signaling, #3661), ACC (1:1000, Cell Signaling, #3662). Secondary mouse or rabbit HRP-conjugated antibodies (1:5000 or 1:10000, Cell Signaling, #7074, #7076) or fluorescently labeled DyLight800 and DyLight680 secondary antibodies (1:5000, Cell Signaling Technology, #5257, 5366, 5470, and 5151) were used. Bands were visualized

using ECL (Pierce West Femto) and images were acquired using the Odyssey Fc Imager (LI-COR Biosciences).

Glucose assay – Mouse aortic smooth muscle cells grown in low or high glucose medium for 7 days. Media was replaced every 48 h. At the end of the last 48h incubation of a 1 week culture, medium was collected and evaluated using the glucose (GO) assay Kit (GAGO-20, Sigma-Aldrich) according to the manufacturer's instructions.

2-deoxyglucose (2-DG) uptake – Mouse aortic smooth muscle cells were cultured in low or high glucose medium for 7 days as described above. Before uptake, cells were rinsed in serum free DMEM and incubated 15 min in 1 µCi/ml ^{3}H-2-DG, room temperature. The uptake was terminated on ice, wherafter cells were solubilized in 1 N NaOH, dissolved in scintillation fluid and subjected to scintillation counting. Cytochalasin B (1 µM) was used to measure non-specific binding.

MTT assay – Mouse aortic smooth muscle cells from passage 3 were plated at a density of $3x10^3$ cells/well in 96-well plates in low glucose (1.7 mM glucose) or high glucose (25 mM glucose) for one week. The cells were subsequently replaced with 100 µl of serum-free DMEM and 10 µl of 3-(4,5-dimethylthiazol-2-yl)-2,5-diphenyl tetrazolium bromide (MTT) solution (5 mg/ml MTT in PBS) for 1 h. The MTT containing medium was removed and the dark blue formazan crystals that formed in intact cells were solubilized with DMSO (100 µl), and the absorbance at 540 nm was measured with a Multiscan GO Microplate Spectrophotometer (Thermo Scientific). Percent cell viability was calculated based on the relative absorbance of treated cells vs cells exposed to the control vehicle.

Calcium measurement **–** Mouse aortic smooth muscle cells were incubated for one week in low (1.7 mM) or high (25 mM) glucose conditions. The culture media was replaced with HEPES-buffered Kreb's solution (in mM : 135.5 NaCl, 5.9 KCl, 2.5 CaCl2, 1.2 MgCl2, 11.6 HEPES, 11.5 glucose; pH 7.4 at 25°C). Following 90 minutes incubation at room temperature with 5µM Fluo-4 (Life Technologies, F-14201) and 0.05% Pluronic-F127, the cells were washed and incubated for a further 30 minutes in HEPES-buffered solution to allow complete de-esterification of intracellular AM esters. Cells were then stimulated in room temperature with 60mM KCl for 7 minutes. Relative changes in calcium levels were recorded using a Zeiss LSM 510 laser-scanning confocal microscope with excitation at 488 nm and emission at 505 nm. Images were acquired every 0.8 s, before and after each stimulation, and changes in global fluorescence (F/F_0) were calculated in confluent cells at the peak and plateau (100-200 seconds after stimulation) response. Baseline fluorescence was evaluated using arbitrary units.

Isometric force measurements

Aortic rings (1.5**–**2 mm in length) were mounted in a Mulvany myograph (610M; Danish Myo Technology) as described previously (31). After an equilibration period, cumulative concentration-responses curves for serotonin (5-HT) were generated. 20µM of the rho-kinase inhibitor Y-27632 was added on top of the highest concentration of 5-HT to evaluate the influence of rho-kinase. The whole experiment was performed in the presence of the nitric oxide synthase inhibitor L-NAME (300 µM).

Adenoviral transduction with MRTF-A - Mouse aortic smooth muscle cells (passage 3 to 5) from wild type and miR-143/145 knockout mice were grown on glass coverslips in 10% FBS, DMEM low or high glucose medium for 1 week. The cells were transduced using cytomegalovirus promoter-driven adenoviral construct: with 100 MOI Ad-hMKL1/eGFP (#ADV-215499, Vector Biolabs) for 96 hr. Following fixation with 4% formaldehyde and permeabilization with 0.1% Triton-X, the nuclei were stained with NucRed Dead 647 (# R37113, Molecular Probes). GFP and nuclear stains were visualized using a Zeiss LSM 510 laser-scanning confocal microscope with excitation at 488 nm and 633 nm. A fixed threshold was set to identify positive nuclei and the ratios of positive vs. total nuclei were then quantified from each condition.

Fluorescence microscopy – Aortae from WT and miR-143/145 KO mice were fixed and sectioned as described previously (32). Sections were stained using calponin primary antibody (Abcam, #ab46784). The staining intensity was determined using a computerized image-analysis system (Olympus CellSens dimension software).

F/G actin assay - Actin polymerization was evaluated using the G-Actin/F-actin In Vivo Assay

Biochem Kit (Cytoskeleton, Inc. #BK037) according to the manufacturer's instructions. Briefly, mouse aortic smooth muscle cells grown in low or high glucose medium were collected in LAS02 lysis buffer (containing ATP and protease inhibitor cocktail). F-actin was pelleted by centrifugation at high speed (100,000 g) using Beckman ultracentrifuge at 37°C for 1 hour. G-actin was transferred to fresh test tubes. F-actin pellet was dissolved in F-actin depolymerizing buffer and incubated on ice for 1 hour. Equal volumes of filamentous and globular actin fraction (10ul) were loaded on the gel. Proteins were transferred to nitrocellulose membrane using Trans Blot Turbo (Bio-Rad) for 10 min at 2.5 A. The membrane was then incubated with rabbit smooth muscle alpha-actin antibody (Cytoskeleton, # AAN01). Anti-rabbit HRP-conjugated secondary antibody (Cell Signaling, #7076 1:10,000) was used. Bands were visualized using ECL (Pierce West Femto) and images were acquired using the Odyssey Fc Imager (LI-COR Biosciences).

Statistics - Values are presented as mean ± S.E.M. unless otherwise stated. Significance analysis of microarrays was done using TMEV v.4.0 software and returned a q value (33). A q value of ≤ 0.1 was considered significant. P-values were calculated by Student's test, one- or two-way analysis of variance (ANOVA) followed by Bonferroni post-hoc testing using GraphPad Prism 5 (GraphPad Software Inc.). $P<0.05$ was considered statistically significant. *, $p<0.05$; **, $p<0.01$; ***, $p<0.001$.

RESULTS

Elevated glucose levels promotes the expression of contractile and cytoskeletal genes in smooth muscle - To evaluate the effects of glucose on smooth muscle differentiation, aortic smooth muscle cells were cultured in low (1.7mM), normal (5.5 mM) and high (25mM) glucose conditions for 1, 3 or 6 weeks. Following 1 week of culture, during which the media was exchanged every 48 hours, the glucose level in the media was slightly reduced to 1.1±0.001 mM in LG and 21.1±0.001 in HG. In accordance with previous observations (34,35), we found that uptake of 2-deoxyglucose glucose uptake was significantly reduced in smooth muscle cells cultured under elevated glucose conditions for one week (fold change in HG vs LG: 0.37±0.11, $p<0.001$, n=5). High versus low glucose levels did not affect cell proliferation or viability measured by the MTT assay (fold change: 1.01.±0.02 in HG vs. LG, $p>0.05$, n=8). Elevating the extracellular glucose concentration for 1 week resulted in increased mRNA expression of several Myocardin/MRTF/SRF regulated contractile markers including calponin (*Cnn1*), Dystrophin (*Dmd*), Desmin (*Des*), SM22 (*Tagln*) and the β_1-subunit of the BK-channel (Figure 1A-E). All of these genes are positively regulated by actin polymerization in smooth muscle cells (36). Coincidently, the expression of the proteoglycan decorin, which is reduced by actin polymerization (36) was decreased by high glucose (Figure 1F).

To test the effect of glucose on genes associated with vascular calcification we analyzed mRNA expression of osteopontin (*Spp1*) and matrix Gla protein (*Mgp*). Expression of *Mgp* was unchanged in HG vs LG conditions (fold change: 0.96±0.05) whereas *Spp1* expression was significantly increased (fold change: 3.82.±0.4, $p<0.001$). Hyperglycemia has previously been demonstrated to activate inflammatory gene expression in endothelial cells (37). However, we did not observe any statistically significant increase in the mRNA expression of either TNF-α (LG: 1.330.±0.41, HG 1.965±0.19, $p>0.05$, n=6) or COX-2 (LG: 1.226.±0.43, HG 2.291±0.38, $p>0.05$, n=6) in smooth muscle cells.

Low glucose with 23.3 mM mannitol had no effect on gene expression, ruling out potential osmotic effects of high glucose. Similar to the effect on mRNA, glucose stimulated protein expression of smooth muscle contractile markers, including SM22, smooth muscle α-actin and calponin (Figure 1G-J). The effect of glucose on these markers was still evident after three weeks in culture (data not shown). Furthermore, *Cnn1* and *Kcnmb1* were significantly elevated at a six week time-point whereas no significant change was observed for *Dmd* (data not shown). Shorter culture periods (48h and 96 hours) had no impact on the expression of contractile smooth muscle markers suggesting that the effects of glucose primarily occur during the end of the one week period (data not shown).

To further define the glucose-dependent transcriptome in smooth muscle cells, cells were

cultured in low and high glucose for two weeks and Affymetrix Gene ST mRNA arrays performed. 491 genes were differentially expressed at the significance level q=0. Four out of five of the most highly upregulated genes (Figure 2A) were known Myocardin/MRTF/SRF regulated contractile markers. Among the five most highly repressed genes (Figure 2B) two (*Sdf2l1* and *Derl3*) play roles in the endoplasmic reticulum stress response, one is a component of the respiratory chain in mitochondria, and one plays a key role in the synthesis of vasoactive H_2S (*Cth*, cystathionine γ-lyase). Genes involved in glucose metabolism via the glycolysis, sorbitol and hexokinase pathways were also evaluated from the microarray data set. However, this analysis did not reveal any clear evidence of up or down-regulation of any of these pathways (data not shown). Using the online tool oPOSSUM (http://opossum.cisreg.ca/), we next identified transcription factors potentially involved in the regulation of the most differentially expressed genes. This in silico approach ranks the rate of occurrence of transcription binding sites in these genes, assigning Z-scores (number of standard deviations above the mean) to each transcription factor; which is normally plotted vs. the GC content of the specified genomic region. As shown in Figure 2C, 15 transcription factors had z-scores higher than 10, and four clearly stood out, suggesting potential functional relevance. These four were Klf4, SRF, SP1 and NFYA. The Affymetrix data also revealed that Klf4 expression was reduced (3-fold, q=0) while Srf expression was increased, suggesting that the effects of glucose on SRF-dependent transcription may be in part due to Klf4 repression and Srf induction (Figure 2D).

In further support of a key role of SRF for the glucose-dependent transcriptional response we found that 18 of the 50 most up-regulated transcripts are confirmed or hypothetical SRF/Myocardin/MRTF regulated genes (Table 1). When comparing the effects of glucose with previous results using the actin stabilizing agent jasplakinolide, we found that 40 of the 100 most up-regulated genes were common for both treatments. In all, these analyses show that Myocardin/MRTF/SRF targets constitute a major transcriptomic signature in vascular smooth muscle cells exposed to high glucose.

Glucose stimulates Rho/Rho-kinase activity in cultured smooth muscle cells - While it is known that glucose can stimulate the activity of Rho leading to inhibition of myosin phosphatase targeting protein (MYPT) and calcium sensitization, the duration of this response has not been thoroughly investigated. In accordance with previous observations (13), we found increased phosphorylation of MYPT after one week of high glucose exposure (Figure 3 A-B). Furthermore, additional Rho-kinase targets such as, LIM-kinase and ezrin/radixin/moesin (ERM) were phosphorylated by glucose (Figure 3C-D). The effect was mainly observed between normal and high glucose levels and the phosphorylation persisted at least for 3 weeks. In addition to Rho-kinase, phosphorylation of MYPT, LIM-kinase and ERM can be regulated by PKC. To determine the activation of PKC by glucose, we used a phospho-(Ser) PKC substrate antibody and found that glucose increased the activity of PKC in smooth muscle (Figure 3F).

LIM-kinase can phosphorylate and inactivate the actin depolymerizing factor cofilin, leading to stabilization of actin filaments. Phosphorylation of cofilin at Ser3 was significantly increased in high compared to low glucose (Figure 3E). Furthermore, using an F/G-actin assay, we found increased actin polymerization after one week of high glucose exposure (Figure 3G).

To confirm the metabolic effects caused by altering extracellular glucose conditions, we next examined the effects of glucose on the AMP-kinase (AMPK) pathway, which is a well-known energy sensor in smooth muscle. As expected, the activating phosphorylation of AMPK and the inhibitory phosphorylation of its downstream substrate acetyl-CoA carboxylase (ACC) were reduced in high glucose conditions.

Collectively, these results support a role for PKC, Rho/Rho-kinase and actin polymerization in the regulation of smooth muscle contractile markers by glucose.

Inhibition of the Rho-actin-MRTF axis reduces glucose-induced expression of smooth muscle contractile markers - In order to identify the importance of the different mediators of the PKC/Rho-actin-MRTF signaling pathway in the response to glucose we used a number of pharmacological inhibitors including the actin depolymerizing agent Latrunculin B (Lat B), the

Rho-kinase inhibitor Y-26732, the PKC inhibitor GF-109203X (GFX) and the MRTF inhibitor CCG-1423. These inhibitors were used during the last 24 hours of a one week incubation in high glucose. We found that the inhibitors completely or partially reversed the high-glucose driven changes in calponin, desmin and dystrophin mRNA (Figure 4A-C). Furthermore, all of the PKC/Rho-actin-MRTF inhibitors reversed the glucose-induced changes in calponin, SM22α and α-actin protein expression (Figure 4D-G). Similar results were obtained after silencing of Rho-kinase or MRTFs using siRNA (Figure 4H).

Activation of smooth muscle markers by glucose is dependent on the miR-143/145 cluster - The miRNAs miR-145 and miR-143 are highly expressed in smooth muscle and transcribed as a bicistronic cluster. MiR-145 is known to regulate smooth muscle contractile differentiation, in part via an effect on Rho-signaling and actin polymerization. We therefore hypothesized that this miRNA cluster could play a role for the effects of glucose in smooth muscle (27,38). To test this hypothesis we analyzed the effect of glucose in smooth muscle cells from WT and miR-143/145 KO mice. Compared to the response in WT cells, the induction of smooth muscle marker expression was essentially lost in miR-143/145 KO smooth muscle cells, both at the mRNA and protein level (Figure 5A-G). Furthermore, this effect correlated with a reduced phosphorylation of mediators in the Rho-signaling pathway (Figure 5H-K).

As demonstrated previously (28), basal expression of smooth muscle marker calponin was slightly reduced in the vascular wall of miR-143/145 KO mice *in situ* (Figure 5L-M). Using GFP-tagged MKL1, we found that HG caused increased nuclear localization (Figure 5N, green: MKL1; red: nuclei). This was not seen in KO mice, arguing that impaired actin regulation by HG in KO mice associates with reduced MKL1 activation.

Calcium influx via L-type calcium channels is involved in the effects of glucose on smooth muscle differentiation – Calcium-influx via L-type calcium channels is an important regulator of Rho-activity and expression of contractile smooth muscle markers (39,40). We therefore analyzed calcium levels in cells under high and low glucose conditions and found that baseline fluorescence of the Fluo-4 calcium indicator was significantly increased in cells subjected to hyperglycemia (Figure 6A). However, although the plateau response tended to be increased in HG vs LG conditions we did not observe a statistically significant difference in either peak (Figure 6B) or plateau responses (Figure 6C) to depolarization with high-KCl.

To test the importance of L-type channels we used the calcium channel inhibitor verapamil which significantly decreased glucose-induced smooth muscle marker expression (Figure 6D-F). Incubation of smooth muscle cells in low glucose with the K_{ATP}-channel inhibitor glibenclamide resulted in the induction of dystrophin mRNA expression to a similar level as with high glucose (Figure 6G). A similar trend was observed with the expression of calponin and desmin but these changes did not reach statistical significance (data not shown). The effect of K_{ATP} channel activation in high glucose conditions was then tested using the K_{ATP} channel opener cromakalim. However, cromakalim had no effect on the glucose-induced mRNA expression of dystrophin (Figure 6G).

Formation of advanced glycation end products (AGE) is crucial for glucose-mediated activation of Rho-signaling and expression of smooth muscle markers.

Activation of the PKC/Rho pathway by hyperglycemia can be mediated by glycated and oxidized proteins and lipids called AGE. To determine the importance of this process for glucose-mediated activation of Rho-signaling and expression of smooth muscle markers we treated smooth muscle cells incubated under high and low glucose conditions with aminoguanidine (AMG), an inhibitor of AGE formation. While AMG had no significant effect in low glucose conditions, it completely prevented the increased expression of contractile smooth muscle markers in high glucose media (Figure 7A-D). Furthermore, this effect correlated with a reduced phosphorylation of mediators in the Rho-signaling pathway including MYPT, ERM and LIMK (Figure 7E-G).

Activation of smooth muscle markers in hyperglycemic mice and diabetic patients - To confirm that glucose can promote smooth muscle differentiation *in vivo*, where baseline expression of smooth muscle markers is already relatively high, we used hyperglycemic Akita mice and analyzed the smooth muscle marker expression

eight weeks after the onset of diabetes. As shown in Figure 8A, mRNA expression of the three smooth muscle markers calponin, dystrophin and desmin were significantly higher in hyperglycemic mice when compared to normoglycemic littermate control WT mice.

We next tested if contractile function was altered in the Akita mice using isometric force measurements of aortas stimulated with the contractile agonist 5-HT. In accordance with previous observations in diabetic animal models (12,41), we found an increased maximal contraction to 5-HT in Akita-mice (Figure 8B). This effect was not dependent on altered NO production as the nitric oxide inhibitor L-NAME was present during the experiment. Approximately 75% of the contraction to 5-HT was mediated by rho-kinase as demonstrated by relaxation to the rho-kinase inhibitor Y-27632 (Figure 8C).

To determine if type-2 diabetes is associated with increased expression of smooth muscle contractile markers, we collected left internal mammary arteries (LIMA) from diabetic (n=6, 100% male) and non-diabetic patients (n=6, 67% male) undergoing coronary artery by-pass grafting (CABG). Their mean age was 68.5±2.6 and 67.8 ± 6.9, for diabetic and non-diabetic, respectively. The gender imbalance reflects the predominance of males undergoing CABG and a greater prevalence of type 2 diabetes in male subjects. Other parameters such as blood pressure, LDL cholesterol and serum creatinine were similar between the groups, while blood glucose levels were significantly increased in the diabetic subjects (Table 2). Elevated blood pressure was treated pharmacologically in both diabetic and non-diabetic patients. The expression of several smooth muscle markers at both mRNA and protein level was higher in the vessels from diabetic patients (Figure 8D-E and G). Furthermore, a significant increase was found in the phosphorylation levels of ERM, LIMK and cofilin suggesting activation of the PKC and/or Rho/Rho-kinase pathway (Figure 8F-G). Collectively, these data suggests that diabetic conditions, possibly via increased extracellular glucose levels, can induce contractile differentiation of smooth muscle cells.

DISCUSSION

In the present study we have demonstrated that PKC/Rho-activation by glucose can promote actin polymerization and expression of contractile and cytoskeletal markers in cultured smooth muscle cells. We also found that this effect is dependent on miR-143/145 expression, PKC/Rho activation and L-type calcium channel signaling. Interestingly, the increased contractile differentiation induced by hyperglycemia appears to be a general effect since the *in vitro* results could be largely recapitulated in hyperglycemic Akita mice and diabetic patients.

Extensive research have suggested that the vascular smooth muscle from diabetic patients and animal models acquire a hyper-contractile phenotype (7-10,12,42,43). Similar effects have been observed in detrusor and airway smooth muscle suggesting a general mechanism for some smooth muscle tissues (44,45). In many cases, the cause of glucose-induced smooth muscle hyper-contractility has been ascribed to an increased PKC/Rho-kinase activity (10,13,14,43,45,46). Increasing levels of glucose cause an elevation in cytosolic calcium levels in vascular smooth muscle (10,47) and both PKC and Rho-activation are in part dependent on intracellular calcium levels (48,49).

In agreement with previous studies, we found that elevated glucose levels increases phosphorylation of specific downstream targets of Rho and/or PKC such as MYPT, ERM, LIMK and cofilin, and caused a general increase in PKC substrate phosphorylation in vascular smooth muscle cells. Glucose-induced signaling events are maintained over several weeks in cell culture, which is an important consideration since this can then result in long-lasting effects on protein expression and remodeling of vascular smooth muscle (18,50). However, an increased PKC/Rho-kinase activity can also directly regulate smooth muscle contractility by inhibition of myosin phosphatase, thereby causing calcium sensitization (51,52). Naturally, other signaling pathways are regulated by glucose in smooth muscle and we cannot exclude their importance for the effects on contractile gene expression in smooth muscle.

High intracellular glucose levels can inhibit the activity of the AMPK-signaling pathway via an increased ATP:AMP ratio. For this to occur, it requires an increased glucose uptake and glucose metabolism in the cells. Since smooth muscle cells mainly express insulin-insensitive GLUT1 transporter (53), glucose transport is limited by the

amount of GLUT1 in the cell membrane. Interestingly, elevated glucose levels resulted in decreased uptake of glucose after one week in culture. This is in accordance with previous observations and can in part be explained by a decreased GLUT1 expression (34,35). However, the decrease in GLUT1 expression is not sufficient to normalize intracellular glucose levels in smooth muscle cells subjected to hyperglycemia (34). To confirm an increased glucose metabolism under hyperglycemic conditions in our model, we analyzed the regulation of AMPK/ACC-signaling and found a significant decrease in AMPK activation under hyperglycemic conditions. However, in both cultured cells and intact blood vessels, activation of AMPK by AICAR results in a significant induction of smooth muscle marker expression (29). Thus, our previous data indicates that the effect of glucose on AMPK would rather counteract glucose-induced expression of contractile smooth muscle markers.

Downstream of Rho/PKC, glucose stimulation increases the F/G-actin ratio in cultured smooth muscle cells, which suggests that actin polymerization is stimulated by hyperglycemia. This may in part be due to a glucose-induced phosphorylation of cofilin. Cofilin belongs to a family of actin depolymerizing factors and is inactivated by phosphorylation by LIM-kinase, leading to increased accumulation of actin filaments (54). Although slower than calcium sensitization, this effect can contribute to acute smooth muscle contractility following Rho-activation (55,56). In accordance with our observation in smooth muscle, F-actin remodeling has been reported to be involved in glucose-induced insulin secretion in pancreatic β-cells, partly via inhibition of cofilin (57).

Concurring with an increased Rho-activation and actin polymerization, we found that glucose promotes the expression of contractile smooth muscle markers at both mRNA and protein levels. If functional contractile filaments are formed from these proteins, this can potentially lead to a sustained augmentation of vascular contractile function and may be an additional mechanism for diabetes-associated hypertension.

The mechanism behind actin-dependent transcription involves nuclear translocation of the transcriptional co-activator MRTF, which is released from monomeric G-actin upon an increased actin polymerization (19). MRTF binds to the serum response factor (SRF) and the resulting ternary complex activates genes that play roles in cytoskeletal organization and contractility (58). SRF binds to genetic elements referred to as CArG boxes and SRF-binding to these genetic elements is inhibited by Kruppel-like factor 4 (Klf4) (20). Here we found that Klf4 is repressed by glucose at the mRNA level arguing that SRF-dependent transcription is not only activated via actin polymerization but also relieved from Klf4-mediated repression. This dual regulation of SRF-dependent transcription is a plausible reason why SRF has such a large, if not dominating, impact on the glucose-dependent transcriptome in smooth muscle. Further work is required to elucidate the mechanism of repression of Klf4 by glucose and its importance in vascular disease. However, it is notable that conditional KO of KLF4 in smooth muscle accelerates neointima formation while maintaining SMC marker expression (59).

A controversial aspect of this study is that diabetes and hyperglycemia are known to exacerbate vascular diseases associated with a synthetic vascular smooth muscle phenotype (i.e. atherosclerosis, restenosis after balloon angioplasty). However, the contractile and synthetic phenotypes of smooth muscle cells are not mutually exclusive as they are regulated by separate intracellular mechanisms (59-61). Thus, pathways leading to increased expression of both contractile and synthetic markers can be activated simultaneously, which seems in line with our finding that osteopontin is simultaneously upregulated with the smooth muscle differentiation markers. Osteopontin is a marker of the synthetic phenotype of smooth muscle, which has been shown to be upregulated in the context of vascular disease, including diabetic vascular complications. In agreement with our results, previous reports have demonstrated that osteopontin is induced by hyperglycemia in smooth muscle cells. Several mechanisms have been proposed including activation of the PKC/Rho-kinase pathway (62) and activation of the transcription factor NFATc3 (63,64). Thus, hyperglycemia in diabetic patients may result in simultaneous activation of the contractile and synthetic gene programs leading to increased risk of neointimal hyperplasia as well as hypertension

and vasospasm. The extent to which these gene programs may be activated may as well vary depending on the vascular bed (i.e. a synthetic program dominance in regions prone to atherosclerosis, a contractile dominance in resistance arteries).

We have previously demonstrated that stretch-induced contractile differentiation in vascular smooth muscle is mediated by increased actin polymerization which is dependent on L-type calcium channel activation and small non-coding RNAs such as miR-145 (23-26,40,65). The regulation of L-type calcium channels expression by miR-145 is in part mediated by direct interaction of miR-145 with its target CamKIIδ (26,66), which in turn affects the translocation of a transcriptional repressor called DREAM (67). In earlier studies, we found that knockdown of miR-145 or genetic deletion of the miR-143/145 cluster results in increased CamKIIδ expression and reduced expression of L-type calcium channels (26,31,68). Considering the sensitivity to L-type calcium channel verapamil, it is likely that reduced L-type calcium channel expression is involved in the diminished glucose-mediated transcription of contractile smooth muscle markers in miR-143/145 KO cells.

It is known that L-type calcium influx can promote (40,69) Rho-signaling and contractile gene expression in smooth muscle. Recent reports suggest that hyperglycemia and diabetes can promote persistent calcium sparklet activity via activation of L-type calcium channels in arterial smooth muscle (70,71). Interestingly, sparklet activity is controlled by PKC and underlies a sustained calcium entry through persistent L-type channel activity (72). In accordance with these findings we found an increased basal Fluo-4 fluorescence following hyperglycemia, which is an indicator of elevated baseline calcium levels in these cells. Relative to baseline levels, the voltage-activated calcium influx was not significantly elevated in hyperglycemic conditions. However, it is likely that the slow and persistent effects that we observe in smooth muscle cells during hyperglycemia require persistent elevations of intracellular calcium levels. This is further supported by our finding that inhibition of L-type calcium channels by verapamil can inhibit glucose-induced smooth muscle differentiation.

The activation of Rho by calcium can either be mediated via PKC and/or the calcium-sensitive proline-rich tyrosine kinase 2 (PYK2) (39,73). In addition to Rho/Rho-kinase, mechanical stress has been demonstrated to activate PKC (74). Thus, glucose and mechanical stimuli share many of the signaling mechanisms leading to increased smooth muscle differentiation. Accordingly, we found that inhibition of PKC/Rho/MRTF signaling and genetic KO of the miR-143/145 cluster reduced glucose-induced contractile gene expression. We cannot exclude some off-target effects of the inhibitors used in this study. However, since siRNAs against Rho-kinases or MRTFs had similar effects as the inhibitors on glucose-induced calponin expression, our results strongly suggest that the PKC/Rho-MRTF pathway is involved in this process.

The most proximal effects of glucose are not fully understood but are thought to involve the formation AGEs. These glycated and oxidized lipids and proteins can be formed both intra- and extra-cellularly and interact with AGE receptors (RAGE) (Reviewed by (75)). In vascular cells, this interaction results in the activation of a number of intracellular pathways including PKC/Rho (76) (16,17). The prototype therapeutic agent aminoguanidine is known to prevent AGE formation by reacting with derivatives of early glycation products such as 3-deoxyglucosone (Reviewed by (77)). Herein, we found that aminoguanidine inhibited activation of Rho-signaling and smooth muscle marker expression induced by glucose but had no effect in low glucose conditions. Our results thus support a major role of AGE for glucose-induced contractile differentiation.

Although AGE formation is a plausible explanation for the effects of glucose on smooth muscle we also tested other possible explanations such as an increased glucose metabolism, which in turn can elevate the levels of ATP in the cells. In pancreatic β-cells, it is well known that glucose-induced calcium influx via voltage gated calcium channels is activated by inhibition of K_{ATP} channels, which is due to an increased ATP production following glucose metabolism. To test if a similar mechanism is possible in smooth muscle cells, we used the K_{ATP} channel inhibitor glibenclamide and the K_{ATP} channel opener cromakalim in the presence of low and high

glucose, respectively. Glibenclamide mimicked the effects of high glucose on contractile marker expression, suggesting that inhibition of K_{ATP} channels is sufficient to induce expression of contractile proteins. However, the lack of any effect of cromakalim in high glucose conditions argues against an important role of K_{ATP} channels for the effects of high glucose on contractile gene expression.

Isolation and culture of vascular smooth muscle cells rapidly results in a phenotypic shift of the cells, which may affect the response observed to a wide variety of stimuli. We thus found it important to test if some of our findings could be recapitulated *in vivo* where baseline expression of contractile smooth muscle markers is several-fold higher compared to the *in vitro* situation. The increased expression of differentiation markers in Akita mice and diabetic patients points toward a general mechanism that may, at least in part, contribute to the hypercontractile phenotype of smooth muscle cells in diabetic conditions. This is in line with previous work which demonstrated increased contractile responses in the vasculature from diabetic patients and hyperglycemic Akita mice (7,78). Our results support these previous observations by demonstrating increased smooth muscle contractions to the vasoactive agonist 5-HT in Akita mice. An increased contraction to 5-HT has been shown in other diabetic animal models and is known to depend on increased activation of the Rho-signaling pathway (12,14,41) However, increased expression of smooth muscle markers does not necessarily result in increased contractility and the increased contractile responses in diabetic animal models can also be mediated by myosin phosphatase inhibition and calcium sensitization. Further studies are thus needed to dissect the exact contribution of glucose-induced transcriptional regulation of contractile genes to force development in smooth muscle *in vivo*.

In diabetic patients, we found that the increase in smooth muscle marker expression correlated with an increased activation of the Rho signaling pathway. This supports the idea that activation of Rho-kinase may be a contributing factor in the development of diabetic vascular disease and that inhibitors of this pathway can be beneficial against cardiovascular complications of diabetes (79-81). However, the mechanism of Rho activation in smooth muscle may differ *in vivo* compared to the *in vitro* situation. *In vivo*, the influence of endothelial cells cannot be excluded and it is thus possible that endothelial dysfunction can contribute to the effects of diabetes that we observe in smooth muscle. Another limitation of this study is the low sample number in the patient study. A larger cohort is needed to verify the changes observed herein and to limit the effects of confounding factors. However, despite a low n-number we were able to detect several significant changes in diabetic patients compared to non-diabetic controls. The low variability between samples can be partly explained by the fact that the patients were relatively well-matched regarding age, sex and blood pressure.

In conclusion, the results of the present study provide evidence for a role of glucose in contractile gene expression in smooth muscle via activation of AGE-, PKC- and Rho-dependent signaling pathways, actin polymerization and Klf4 repression. Altogether, these data suggest a novel possible mechanism for the development of diabetic vascular diseases and provide further support for the potential therapeutic use of Rho-kinase inhibitors in these conditions.

CONFLICT OF INTEREST

The authors declare that they have no conflicts of interest with the contents of this article.

AUTHOR CONTRIBUTIONS

All authors have critically revised the manuscript and approved its submission. TTH, KSw, MFG, KSt and SA have contributed to the conception and design of the experiments, drafting the manuscript and interpretation of data. TTH, KMT, DD, ME, MFG, JS, JN, TBr, TBo, KSt, KSw, SA and EGV have contributed to the acquisition and analysis of data.

REFERENCES

1. Hossain, P., Kawar, B., and El Nahas, M. (2007) Obesity and diabetes in the developing world--a growing challenge. *N Engl J Med* **356**, 213-215
2. Sarwar, N., Gao, P., Seshasai, S. R., Gobin, R., Kaptoge, S., Di Angelantonio, E., Ingelsson, E., Lawlor, D. A., Selvin, E., Stampfer, M., Stehouwer, C. D., Lewington, S., Pennells, L., Thompson, A., Sattar, N., White, I. R., Ray, K. K., and Danesh, J. (2010) Diabetes mellitus, fasting blood glucose concentration, and risk of vascular disease: a collaborative meta-analysis of 102 prospective studies. *Lancet* **375**, 2215-2222
3. Coutinho, M., Gerstein, H. C., Wang, Y., and Yusuf, S. (1999) The relationship between glucose and incident cardiovascular events. A metaregression analysis of published data from 20 studies of 95,783 individuals followed for 12.4 years. *Diabetes Care* **22**, 233-240
4. Lawes, C. M., Parag, V., Bennett, D. A., Suh, I., Lam, T. H., Whitlock, G., Barzi, F., and Woodward, M. (2004) Blood glucose and risk of cardiovascular disease in the Asia Pacific region. *Diabetes Care* **27**, 2836-2842
5. Thomas, M. C. (2014) Glycemic exposure, glycemic control, and metabolic karma in diabetic complications. *Adv Chronic Kidney Dis* **21**, 311-317
6. Goldberg, I. J. (2004) Why does diabetes increase atherosclerosis? I don't know! *J Clin Invest* **114**, 613-615
7. Fleischhacker, E., Esenabhalu, V. E., Spitaler, M., Holzmann, S., Skrabal, F., Koidl, B., Kostner, G. M., and Graier, W. F. (1999) Human diabetes is associated with hyperreactivity of vascular smooth muscle cells due to altered subcellular Ca2+ distribution. *Diabetes* **48**, 1323-1330
8. White, R. E., and Carrier, G. O. (1988) Enhanced vascular alpha-adrenergic neuroeffector system in diabetes: importance of calcium. *Am J Physiol* **255**, H1036-1042
9. Abebe, W., Harris, K. H., and MacLeod, K. M. (1990) Enhanced contractile responses of arteries from diabetic rats to alpha 1-adrenoceptor stimulation in the absence and presence of extracellular calcium. *J Cardiovasc Pharmacol* **16**, 239-248
10. Ungvari, Z., Pacher, P., Kecskemeti, V., Papp, G., Szollar, L., and Koller, A. (1999) Increased myogenic tone in skeletal muscle arterioles of diabetic rats. Possible role of increased activity of smooth muscle Ca2+ channels and protein kinase C. *Cardiovasc Res* **43**, 1018-1028
11. Creager, M. A., Luscher, T. F., Cosentino, F., and Beckman, J. A. (2003) Diabetes and vascular disease: pathophysiology, clinical consequences, and medical therapy: Part I. *Circulation* **108**, 1527-1532
12. Guo, Z., Su, W., Allen, S., Pang, H., Daugherty, A., Smart, E., and Gong, M. C. (2005) COX-2 up-regulation and vascular smooth muscle contractile hyperreactivity in spontaneous diabetic db/db mice. *Cardiovasc Res* **67**, 723-735
13. Xie, Z., Su, W., Guo, Z., Pang, H., Post, S. R., and Gong, M. C. (2006) Up-regulation of CPI-17 phosphorylation in diabetic vasculature and high glucose cultured vascular smooth muscle cells. *Cardiovasc Res* **69**, 491-501
14. Xie, Z., Gong, M. C., Su, W., Xie, D., Turk, J., and Guo, Z. (2010) Role of calcium-independent phospholipase A2beta in high glucose-induced activation of RhoA, Rho kinase, and CPI-17 in cultured vascular smooth muscle cells and vascular smooth muscle hypercontractility in diabetic animals. *J Biol Chem* **285**, 8628-8638
15. Cicek, F. A., Kandilci, H. B., and Turan, B. (2013) Role of ROCK upregulation in endothelial and smooth muscle vascular functions in diabetic rat aorta. *Cardiovasc Diabetol* **12**, 51
16. Bu, D. X., Rai, V., Shen, X., Rosario, R., Lu, Y., D'Agati, V., Yan, S. F., Friedman, R. A., Nuglozeh, E., and Schmidt, A. M. (2010) Activation of the ROCK1 branch of the transforming growth factor-

beta pathway contributes to RAGE-dependent acceleration of atherosclerosis in diabetic ApoE-null mice. *Circ Res* **106**, 1040-1051
17. Thallas-Bonke, V., Lindschau, C., Rizkalla, B., Bach, L. A., Boner, G., Meier, M., Haller, H., Cooper, M. E., and Forbes, J. M. (2004) Attenuation of extracellular matrix accumulation in diabetic nephropathy by the advanced glycation end product cross-link breaker ALT-711 via a protein kinase C-alpha-dependent pathway. *Diabetes* **53**, 2921-2930
18. Mack, C. P., Somlyo, A. V., Hautmann, M., Somlyo, A. P., and Owens, G. K. (2001) Smooth muscle differentiation marker gene expression is regulated by RhoA-mediated actin polymerization. *J Biol Chem* **276**, 341-347
19. Miralles, F., Posern, G., Zaromytidou, A. I., and Treisman, R. (2003) Actin dynamics control SRF activity by regulation of its coactivator MAL. *Cell* **113**, 329-342
20. Liu, Y., Sinha, S., McDonald, O. G., Shang, Y., Hoofnagle, M. H., and Owens, G. K. (2005) Kruppel-like factor 4 abrogates myocardin-induced activation of smooth muscle gene expression. *J Biol Chem* **280**, 9719-9727
21. Albinsson, S., and Hellstrand, P. (2007) Integration of signal pathways for stretch-dependent growth and differentiation in vascular smooth muscle. *Am J Physiol Cell Physiol* **293**, C772-782
22. Hellstrand, P., and Albinsson, S. (2005) Stretch-dependent growth and differentiation in vascular smooth muscle: role of the actin cytoskeleton. *Canadian journal of physiology and pharmacology* **83**, 869-875
23. Albinsson, S., Nordstrom, I., and Hellstrand, P. (2004) Stretch of the vascular wall induces smooth muscle differentiation by promoting actin polymerization. *J Biol Chem* **279**, 34849-34855
24. Zeidan, A., Nordstrom, I., Albinsson, S., Malmqvist, U., Sward, K., and Hellstrand, P. (2003) Stretch-induced contractile differentiation of vascular smooth muscle: sensitivity to actin polymerization inhibitors. *Am J Physiol Cell Physiol* **284**, C1387-1396
25. Turczynska, K. M., Hellstrand, P., Sward, K., and Albinsson, S. (2013) Regulation of vascular smooth muscle mechanotransduction by microRNAs and L-type calcium channels. *Commun Integr Biol* **6**, e22278
26. Turczynska, K. M., Sadegh, M. K., Hellstrand, P., Sward, K., and Albinsson, S. (2012) MicroRNAs are essential for stretch-induced vascular smooth muscle contractile differentiation via microRNA (miR)-145-dependent expression of L-type calcium channels. *J Biol Chem* **287**, 19199-19206
27. Albinsson, S., Suarez, Y., Skoura, A., Offermanns, S., Miano, J. M., and Sessa, W. C. (2010) MicroRNAs are necessary for vascular smooth muscle growth, differentiation, and function. *Arterioscler Thromb Vasc Biol* **30**, 1118-1126
28. Boettger, T., Beetz, N., Kostin, S., Schneider, J., Kruger, M., Hein, L., and Braun, T. (2009) Acquisition of the contractile phenotype by murine arterial smooth muscle cells depends on the Mir143/145 gene cluster. *J Clin Invest* **119**, 2634-2647
29. Turczynska, K. M., Bhattachariya, A., Sall, J., Goransson, O., Sward, K., Hellstrand, P., and Albinsson, S. (2013) Stretch-Sensitive Down-Regulation of the miR-144/451 Cluster in Vascular Smooth Muscle and Its Role in AMP-Activated Protein Kinase Signaling. *PLoS One* **8**, e65135
30. Sadegh, M. K., Ekman, M., Rippe, C., Uvelius, B., Sward, K., and Albinsson, S. (2012) Deletion of dicer in smooth muscle affects voiding pattern and reduces detrusor contractility and neuroeffector transmission. *PLoS One* **7**, e35882
31. Dahan, D., Ekman, M., Larsson-Callerfelt, A. K., Turczynska, K., Boettger, T., Braun, T., Sward, K., and Albinsson, S. (2014) Induction of angiotensin-converting enzyme after miR-143/145 deletion is critical for impaired smooth muscle contractility. *Am J Physiol Cell Physiol* **307**, C1093-1101

32. Dahan, D., Ekman, M., Larsson-Callerfelt, A. K., Turczynska, K., Boettger, T., Braun, T., Sward, K., and Albinsson, S. (2014) Induction of angiotensin converting enzyme after miR-143/145 deletion is critical for impaired smooth muscle contractility. *Am J Physiol Cell Physiol*
33. Storey, J. D., and Tibshirani, R. (2003) Statistical significance for genomewide studies. *Proc Natl Acad Sci U S A* **100**, 9440-9445
34. Howard, R. L. (1996) Down-regulation of glucose transport by elevated extracellular glucose concentrations in cultured rat aortic smooth muscle cells does not normalize intracellular glucose concentrations. *J Lab Clin Med* **127**, 504-515
35. Kaiser, N., Sasson, S., Feener, E. P., Boukobza-Vardi, N., Higashi, S., Moller, D. E., Davidheiser, S., Przybylski, R. J., and King, G. L. (1993) Differential regulation of glucose transport and transporters by glucose in vascular endothelial and smooth muscle cells. *Diabetes* **42**, 80-89
36. Turczynska, K. M., Sward, K., Hien, T. T., Wohlfahrt, J., Mattisson, I. Y., Ekman, M., Nilsson, J., Sjogren, J., Murugesan, V., Hultgardh-Nilsson, A., Cidad, P., Hellstrand, P., Perez-Garcia, M. T., and Albinsson, S. (2015) Regulation of smooth muscle dystrophin and synaptopodin 2 expression by actin polymerization and vascular injury. *Arterioscler Thromb Vasc Biol* **35**, 1489-1497
37. Cosentino, F., Eto, M., De Paolis, P., van der Loo, B., Bachschmid, M., Ullrich, V., Kouroedov, A., Delli Gatti, C., Joch, H., Volpe, M., and Luscher, T. F. (2003) High glucose causes upregulation of cyclooxygenase-2 and alters prostanoid profile in human endothelial cells: role of protein kinase C and reactive oxygen species. *Circulation* **107**, 1017-1023
38. Xin, M., Small, E. M., Sutherland, L. B., Qi, X., McAnally, J., Plato, C. F., Richardson, J. A., Bassel-Duby, R., and Olson, E. N. (2009) MicroRNAs miR-143 and miR-145 modulate cytoskeletal dynamics and responsiveness of smooth muscle cells to injury. *Genes Dev* **23**, 2166-2178
39. Ying, Z., Giachini, F. R., Tostes, R. C., and Webb, R. C. (2009) PYK2/PDZ-RhoGEF links Ca2+ signaling to RhoA. *Arterioscler Thromb Vasc Biol* **29**, 1657-1663
40. Ren, J., Albinsson, S., and Hellstrand, P. (2010) Distinct effects of voltage- and store-dependent calcium influx on stretch-induced differentiation and growth in vascular smooth muscle. *J Biol Chem* **285**, 31829-31839
41. Matsumoto, T., Kobayashi, T., Ishida, K., Taguchi, K., and Kamata, K. (2010) Enhancement of mesenteric artery contraction to 5-HT depends on Rho kinase and Src kinase pathways in the ob/ob mouse model of type 2 diabetes. *Br J Pharmacol* **160**, 1092-1104
42. Nobe, K., Sakai, Y., Maruyama, Y., and Momose, K. (2002) Hyper-reactivity of diacylglycerol kinase is involved in the dysfunction of aortic smooth muscle contractility in streptozotocin-induced diabetic rats. *Br J Pharmacol* **136**, 441-451
43. Kizub, I. V., Pavlova, O. O., Johnson, C. D., Soloviev, A. I., and Zholos, A. V. (2010) Rho kinase and protein kinase C involvement in vascular smooth muscle myofilament calcium sensitization in arteries from diabetic rats. *Br J Pharmacol* **159**, 1724-1731
44. Chang, S., Hypolite, J. A., DiSanto, M. E., Changolkar, A., Wein, A. J., and Chacko, S. (2006) Increased basal phosphorylation of detrusor smooth muscle myosin in alloxan-induced diabetic rabbit is mediated by upregulation of Rho-kinase beta and CPI-17. *Am J Physiol Renal Physiol* **290**, F650-656
45. Cazzola, M., Calzetta, L., Rogliani, P., Lauro, D., Novelli, L., Page, C. P., Kanabar, V., and Matera, M. G. (2012) High glucose enhances responsiveness of human airways smooth muscle via the Rho/ROCK pathway. *Am J Respir Cell Mol Biol* **47**, 509-516
46. Lee, T. S., Saltsman, K. A., Ohashi, H., and King, G. L. (1989) Activation of protein kinase C by elevation of glucose concentration: proposal for a mechanism in the development of diabetic vascular complications. *Proc Natl Acad Sci U S A* **86**, 5141-5145

47. Barbagallo, M., Shan, J., Pang, P. K., and Resnick, L. M. (1995) Glucose-induced alterations of cytosolic free calcium in cultured rat tail artery vascular smooth muscle cells. *J Clin Invest* **95**, 763-767
48. Sakurada, S., Takuwa, N., Sugimoto, N., Wang, Y., Seto, M., Sasaki, Y., and Takuwa, Y. (2003) Ca2+-dependent activation of Rho and Rho kinase in membrane depolarization-induced and receptor stimulation-induced vascular smooth muscle contraction. *Circ Res* **93**, 548-556
49. Luo, J. H., and Weinstein, I. B. (1993) Calcium-dependent activation of protein kinase C. The role of the C2 domain in divalent cation selectivity. *J Biol Chem* **268**, 23580-23584
50. Staiculescu, M. C., Galinanes, E. L., Zhao, G., Ulloa, U., Jin, M., Beig, M. I., Meininger, G. A., and Martinez-Lemus, L. A. (2013) Prolonged vasoconstriction of resistance arteries involves vascular smooth muscle actin polymerization leading to inward remodelling. *Cardiovasc Res* **98**, 428-436
51. Kimura, K., Ito, M., Amano, M., Chihara, K., Fukata, Y., Nakafuku, M., Yamamori, B., Feng, J., Nakano, T., Okawa, K., Iwamatsu, A., and Kaibuchi, K. (1996) Regulation of myosin phosphatase by Rho and Rho-associated kinase (Rho-kinase). *Science* **273**, 245-248
52. Masuo, M., Reardon, S., Ikebe, M., and Kitazawa, T. (1994) A novel mechanism for the Ca(2+)-sensitizing effect of protein kinase C on vascular smooth muscle: inhibition of myosin light chain phosphatase. *J Gen Physiol* **104**, 265-286
53. Pyla, R., Poulose, N., Jun, J. Y., and Segar, L. (2013) Expression of conventional and novel glucose transporters, GLUT1, -9, -10, and -12, in vascular smooth muscle cells. *Am J Physiol Cell Physiol* **304**, C574-589
54. Arber, S., Barbayannis, F. A., Hanser, H., Schneider, C., Stanyon, C. A., Bernard, O., and Caroni, P. (1998) Regulation of actin dynamics through phosphorylation of cofilin by LIM-kinase. *Nature* **393**, 805-809
55. Moreno-Dominguez, A., Colinas, O., El-Yazbi, A., Walsh, E. J., Hill, M. A., Walsh, M. P., and Cole, W. C. (2013) Ca2+ sensitization due to myosin light chain phosphatase inhibition and cytoskeletal reorganization in the myogenic response of skeletal muscle resistance arteries. *J Physiol* **591**, 1235-1250
56. Mehta, D., and Gunst, S. J. (1999) Actin polymerization stimulated by contractile activation regulates force development in canine tracheal smooth muscle. *J Physiol (Lond)* **519**, 829-840
57. Uenishi, E., Shibasaki, T., Takahashi, H., Seki, C., Hamaguchi, H., Yasuda, T., Tatebe, M., Oiso, Y., Takenawa, T., and Seino, S. (2013) Actin dynamics regulated by the balance of neuronal Wiskott-Aldrich syndrome protein (N-WASP) and cofilin activities determines the biphasic response of glucose-induced insulin secretion. *J Biol Chem* **288**, 25851-25864
58. Miano, J. M., Long, X., and Fujiwara, K. (2007) Serum response factor: master regulator of the actin cytoskeleton and contractile apparatus. *Am J Physiol Cell Physiol* **292**, C70-81
59. Yoshida, T., Kaestner, K. H., and Owens, G. K. (2008) Conditional deletion of Kruppel-like factor 4 delays downregulation of smooth muscle cell differentiation markers but accelerates neointimal formation following vascular injury. *Circ Res* **102**, 1548-1557
60. Shi, N., and Chen, S. Y. (2014) Mechanisms simultaneously regulate smooth muscle proliferation and differentiation. *J Biomed Res* **28**, 40-46
61. Rama, A., Matsushita, T., Charolidi, N., Rothery, S., Dupont, E., and Severs, N. J. (2006) Up-regulation of connexin43 correlates with increased synthetic activity and enhanced contractile differentiation in TGF-beta-treated human aortic smooth muscle cells. *Eur J Cell Biol* **85**, 375-386
62. Kawamura, H., Yokote, K., Asaumi, S., Kobayashi, K., Fujimoto, M., Maezawa, Y., Saito, Y., and Mori, S. (2004) High glucose-induced upregulation of osteopontin is mediated via Rho/Rho kinase pathway in cultured rat aortic smooth muscle cells. *Arterioscler Thromb Vasc Biol* **24**, 276-281

63. Nilsson-Berglund, L. M., Zetterqvist, A. V., Nilsson-Ohman, J., Sigvardsson, M., Gonzalez Bosc, L. V., Smith, M. L., Salehi, A., Agardh, E., Fredrikson, G. N., Agardh, C. D., Nilsson, J., Wamhoff, B. R., Hultgardh-Nilsson, A., and Gomez, M. F. (2010) Nuclear factor of activated T cells regulates osteopontin expression in arterial smooth muscle in response to diabetes-induced hyperglycemia. *Arterioscler Thromb Vasc Biol* **30**, 218-224
64. Zetterqvist, A. V., Berglund, L. M., Blanco, F., Garcia-Vaz, E., Wigren, M., Duner, P., Andersson, A. M., To, F., Spegel, P., Nilsson, J., Bengtsson, E., and Gomez, M. F. (2014) Inhibition of nuclear factor of activated T-cells (NFAT) suppresses accelerated atherosclerosis in diabetic mice. *PLoS One* **8**, e65020
65. Bhattachariya, A., Dahan, D., Ekman, M., Boettger, T., Braun, T., Sward, K., Hellstrand, P., and Albinsson, S. (2015) Spontaneous activity and stretch-induced contractile differentiation are reduced in vascular smooth muscle of miR-143/145 knockout mice. *Acta Physiol (Oxf)*
66. Cordes, K. R., Sheehy, N. T., White, M. P., Berry, E. C., Morton, S. U., Muth, A. N., Lee, T. H., Miano, J. M., Ivey, K. N., and Srivastava, D. (2009) miR-145 and miR-143 regulate smooth muscle cell fate and plasticity. *Nature* **460**, 705-710
67. Ronkainen, J. J., Hanninen, S. L., Korhonen, T., Koivumaki, J. T., Skoumal, R., Rautio, S., Ronkainen, V. P., and Tavi, P. (2011) Ca2+-calmodulin-dependent protein kinase II represses cardiac transcription of the L-type calcium channel alpha(1C)-subunit gene (Cacna1c) by DREAM translocation. *J Physiol* **589**, 2669-2686
68. Bhattachariya, A., Dahan, D., Ekman, M., Boettger, T., Braun, T., Sward, K., Hellstrand, P., and Albinsson, S. (2015) Spontaneous activity and stretch-induced contractile differentiation are reduced in vascular smooth muscle of miR-143/145 knockout mice. *Acta Physiol (Oxf)* **215**, 133-143
69. Wamhoff, B. R., Bowles, D. K., McDonald, O. G., Sinha, S., Somlyo, A. P., Somlyo, A. V., and Owens, G. K. (2004) L-type voltage-gated Ca2+ channels modulate expression of smooth muscle differentiation marker genes via a rho kinase/myocardin/SRF-dependent mechanism. *Circ Res* **95**, 406-414
70. Nystoriak, M. A., Nieves-Cintron, M., Nygren, P. J., Hinke, S. A., Nichols, C. B., Chen, C. Y., Puglisi, J. L., Izu, L. T., Bers, D. M., Dell'acqua, M. L., Scott, J. D., Santana, L. F., and Navedo, M. F. (2014) AKAP150 contributes to enhanced vascular tone by facilitating large-conductance Ca2+-activated K+ channel remodeling in hyperglycemia and diabetes mellitus. *Circ Res* **114**, 607-615
71. Navedo, M. F., Takeda, Y., Nieves-Cintron, M., Molkentin, J. D., and Santana, L. F. (2010) Elevated Ca2+ sparklet activity during acute hyperglycemia and diabetes in cerebral arterial smooth muscle cells. *Am J Physiol Cell Physiol* **298**, C211-220
72. Navedo, M. F., Amberg, G. C., Votaw, V. S., and Santana, L. F. (2005) Constitutively active L-type Ca2+ channels. *Proc Natl Acad Sci U S A* **102**, 11112-11117
73. Kandabashi, T., Shimokawa, H., Miyata, K., Kunihiro, I., Eto, Y., Morishige, K., Matsumoto, Y., Obara, K., Nakayama, K., Takahashi, S., and Takeshita, A. (2003) Evidence for protein kinase C-mediated activation of Rho-kinase in a porcine model of coronary artery spasm. *Arterioscler Thromb Vasc Biol* **23**, 2209-2214
74. Li, C., Wernig, F., Leitges, M., Hu, Y., and Xu, Q. (2003) Mechanical stress-activated PKCdelta regulates smooth muscle cell migration. *FASEB J* **17**, 2106-2108
75. Singh, R., Barden, A., Mori, T., and Beilin, L. (2001) Advanced glycation end-products: a review. *Diabetologia* **44**, 129-146
76. Hirose, A., Tanikawa, T., Mori, H., Okada, Y., and Tanaka, Y. (2010) Advanced glycation end products increase endothelial permeability through the RAGE/Rho signaling pathway. *Febs Lett* **584**, 61-66

77. Goldin, A., Beckman, J. A., Schmidt, A. M., and Creager, M. A. (2006) Advanced glycation end products: sparking the development of diabetic vascular injury. *Circulation* **114**, 597-605
78. Yang, X. Q., Wang, Y. Y., and Chen, A. F. (2008) Increased superoxide contributes to enhancement of vascular contraction in Ins2(Akita) diabetic mice, an autosomal dominant mutant model. *Clin Exp Pharmacol Physiol* **35**, 1097-1103
79. Yao, L., Chandra, S., Toque, H. A., Bhatta, A., Rojas, M., Caldwell, R. B., and Caldwell, R. W. (2013) Prevention of diabetes-induced arginase activation and vascular dysfunction by Rho kinase (ROCK) knockout. *Cardiovasc Res* **97**, 509-519
80. Arita, R., Hata, Y., Nakao, S., Kita, T., Miura, M., Kawahara, S., Zandi, S., Almulki, L., Tayyari, F., Shimokawa, H., Hafezi-Moghadam, A., and Ishibashi, T. (2009) Rho kinase inhibition by fasudil ameliorates diabetes-induced microvascular damage. *Diabetes* **58**, 215-226
81. Lin, G., Craig, G. P., Zhang, L., Yuen, V. G., Allard, M., McNeill, J. H., and MacLeod, K. M. (2007) Acute inhibition of Rho-kinase improves cardiac contractile function in streptozotocin-diabetic rats. *Cardiovasc Res* **75**, 51-58

Acknowledgements **-** We acknowledge the SCIBLU core facility at Lund University and Dr. S. Veerla for carrying out the microarray analyses.

FOOTNOTES

*****This work was supported by the Novo Nordisk Foundation and the Albert Påhlsson foundation to S.A. Also by grants from the Swedish Heart and Lung Foundation (HLF 20130700), the Swedish Research Council (2014-3352) and the Swedish Diabetes Association (Diabetesfonden) to M.F.G and K.St. This work was also supported by Innovative Medicines Initiative Joint Undertaking [#115006], comprising funds from the European Union's Seventh Framework Programme [FP7/2007-2013] and EFPIA companies' in kind contribution.

[1] To whom correspondence should be addressed: Sebastian Albinsson, Department of Experimental Medical Science, Lund University, BMC D12, SE-221 84 Lund, Sweden, Tel: +46-46-2227765, Fax: +46-46-2113417, E-mail: sebastian.albinsson@med.lu.se
[2] Department of Clinical Sciences, Lund University, Sweden
[3]Max Planck Institute for Heart and Lung Research, Bad Nauheim, Germany
[4] Department of Clinical Sciences in Malmö, Lund University, Sweden
[5]Abbreviations: ERM Ezrin/Radixin/Moesin; GFX, GF 109203X; KLF4, Kruppel-like factor 4; LIMA, Left Internal Mammary Artery; LIMK, LIM kinase; MRTF, Myocardin related transcription factor; MYPT, myosin phosphatase; NO, nitric oxide; PKC, Protein Kinase C; PYK2, proline-rich tyrosine kinase 2; SRF, serum response factor; VSMC, vascular smooth muscle cell

Figure legends

Table 1 Microarray analysis of glucose-induced transcripts reveal enrichment of SRF/MRTF/Myocd regulated genes. Aortic smooth muscle cells were cultured for 1 week under high or low glucose conditions. The table displays the 50 most upregulated genes identified by gene array. Known or hypothetical MRTF/Myocd-regulated genes are shown in bold. *Myocd dependent but SRF-independent.

Table 2 Clinical characteristics of LIMA donors. Clinical characteristics were obtained pre-operation for patients undergoing coronary artery bypass graft surgery (n=4-6 patients).

Figure 1. Glucose promotes the expression of contractile smooth muscle markers. Aortic smooth muscle cells were incubated in low (1.7mM; LG), normal (5.5mM; NG) and high (25mM; HG) glucose conditions for one week. Mannitol (Man) was used as osmotic control. The expression of smooth muscle markers was analyzed at the mRNA level by qPCR (A-F; n=3-7) and at the protein level by western blotting (G-J; n=5-6). Gene symbols: calponin, *Cnn1*; dystrophin, *Dmd*; desmin, *Des*; β1-subunit of BK channel, *Kcnmb1*; SM22, *Tagln*; decorin, *Dcn.* *, $p<0.05$; **, $p<0.01$; ***, $p<0.001$ relative to LG.

Figure 2. Glucose-induced SRF-dependent gene expression in vascular smooth muscle. Gene expression induced by culture of smooth muscle cells in high (HG) versus low glucose (LG) was analyzed using Affymterix microarrays (n=6). The genes with the largest relative fold induction and repression are shown in panels A and B, respectively. Significance Analysis of Microarrays (SAM) was used to calculate q-values and $q\leq0.1$ was considered significant. Panel C is a graphic representation of a transcription factor binding site analysis. SRF, Klf4, SP1 and NFYA (highlighted by rings) motifs were enriched ±5 kbases of the transcription start sites of the HG gene set (q=0) as indicated by Z-scores deviating more than 2 standard deviations from the mean. Panel D shows expression of Klf4, Myocd, Mkl1 and SRF from the arrays.

Figure 3. Activation of PKC/Rho signaling by hyperglycemia. Aortic smooth muscle cells were cultured for one week in low (1.7mM; LG), normal (5.5mM; NG) and high (25mM; HG) glucose conditions were analyzed by western blotting using phospho-specific antibodies (A-F; H-I; n=3-5). Actin polymerization was evaluated using an ultracentrifugation assay and the F/G actin ratio was determined by western blotting (G; n=4). Abbreviations: myosin phosphatase targeting protein; MYPT, ezrin, radixin and moesin; ERM, LIM-kinase; LIMK, Mannitol; Man; AMP-activated protein kinase; AMPK, Acetyl-CoA carboxylase; ACC. *, $p<0.05$; **, $p<0.01$; ***, $p<0.001$ relative to LG or as indicated by lines.

Figure 4. Inhibition of the PKC/Rho pathway reverses the effects of glucose on smooth muscle differentiation. Smooth muscle cells were incubated with low (LG) or high (HG) glucose for 1 week with inhibitors present during the last 24 hours. Expression of smooth muscle markers was analyzed by qPCR (A-C; n=4-6) or western blotting (D-G; n=3). Calponin expression was analyzed by qPCR following transfection of smooth muscle cells with siRNA against MKL1, MKL2, ROCK1, ROCK2 or MKL1/2 or ROCK1/2 in combination (H; n=3-6). Abbreviations: LatB, Latrunculin B (causes actin depolymerization); Y-, Y-27632 (Rho-kinase inhibitor); CCG, CCG-1423 (MKL/MRTF inhibitor); GFX, GF 109203X (PKC inhibitor); Ver, Verapamil (L-type channel inhibitor). Gene symbols: calponin, *Cnn1*; dystrophin, *Dmd*; desmin, *Des; MKL1/2*, MRTF-A/B; *ROCK1/2*, Rho-kinase. *, $p<0.05$; **, $p<0.01$; ***, $p<0.001$ relative to LG or relative to HG (#).

Figure 5. Expression of the miR-143/145 cluster is essential for the effects of glucose on smooth muscle differentiation. Aortic smooth muscle cells from three to four miR-143/145 knockout (KO) and littermate wild type (WT) mice were incubated for 1 week under low (LG) or high (HG) glucose conditions. Expression of contractile smooth muscle markers was determined at the mRNA (A-C; n=4-6) and protein (D-G; n=4) level using qPCR and western blotting, respectively. Phosphorylation of mediators in the Rho-signaling pathway was evaluated using phospho-specific antibodies and western blotting (H-K; myosin phosphatase targeting protein; MYPT, ezrin, radixin and moesin; ERM, LIM-kinase; LIMK). Immunofluorescence staining for calponin (red) in WT and miR-143/145 KO aortae (L-M). WT and mir-143/134 KO smooth muscle cells were cultured in low or high glucose conditions for one week and transduced with ad-MKL1/eGFP for 96 hours (N). The nuclear accumulation of MKL1

(green) was analyzed by confocal microscopy and compared with the total number of nuclei (red). Gene symbols: calponin, *Cnn1*; dystrophin, *Dmd*; desmin, *Des*. *, p<0.05; **, p<0.01; ***, p<0.001.

Figure 6. Calcium influx via L-type calcium channels is involved in the effect of glucose on smooth muscle differentiation. Following 1 week incubation under low (LG) or high (HG) glucose conditions, intracellula calcium levels were analyzed using the calcium indicator Fluo-4. Baseline fluorescence (A), peak response to 60 mM KCl (B) and plateau levels following KCl stimulation (C) were evaluated. Smooth muscle cells were incubated with LG or HG for one week with verapamil present during the last 24 hours. Expression of smooth muscle markers was analyzed by qPCR (D-F; n=6). G, qPCR analysis of smooth muscle cells cultured for one week under low glucose conditions in the presence of the K_{ATP}-channel inhibitior glibenclamide (Glib) or in high glucose in the presence of the K_{ATP}-channel opener cromakalim (Crom)(n=4-6). Gene symbols: calponin, *Cnn1*; dystrophin, *Dmd*; desmin, *Des*. *, p<0.05; **, p<0.01; ***, p<0.001 relative to LG or as indicated by lines.

Figure 7. Formation of advanced glycation endproducts (AGE) play a crucial role for glucose-mediated effects in smooth muscle. Smooth muscle cells were incubated with low (LG) or high (HG) glucose for one week with AMG 100 μM present during the last 24 hours**.** Expression of contractile smooth muscle markers was determined at the protein level (A-D; n=4) by western blotting. Phosphorylation of mediators in the Rho-signaling pathway was evaluated using phospho-specific antibodies and western blotting (H-K; myosin phosphatase targeting protein; MYPT, ezrin, radixin and moesin; ERM, LIM-kinase; LIMK). *, p<0.05; **, p<0.01; ***, p<0.001.

Figure 8. Expression of contractile smooth muscle markers is increased in vessels from hyperglycemic mice and diabetic patients. Expression of contractile smooth muscle markers was analyzed by qPCR in small mesenteric arteries from hyperglycemic Akita mice (A; n=5-6). Contractile responses to 5-HT was determined using isometric force measurement of thoracic aorta from WT and Akita mice (B; n=4). The influence of rho-kinase on 5-HT contractions was determined using the rho-kinase inhibitor Y-27632 (C). Smooth muscle marker expression in left internal mammary arteries (LIMA) from diabetic (Dia) and non-diabetic (Non-dia) patients was analyzed qPCR (D) and western blotting (E,G). Protein phosphorylation of mediators in the Rho/Rho-kinase pathway was determined by western blotting using phosphospecific antibodies (F,G) (n=6). *, p<0.05; **, p<0.01; ***, p<0.001 relative to WT or Non-dia.

Table 1

Gene Symbol	Gene Description	T-test(p-value)	Fold Change	q-value (%)
Acta1	**actin, alpha 1, skeletal muscle**	**7,63E-08**	**8,596519**	**0**
Myh11	**myosin, heavy polypeptide 11, smooth muscle**	**3,64E-05**	**8,130582**	**0**
Actg2	**actin, gamma 2, smooth muscle, enteric**	**4,13E-04**	**6,7903028**	**0**
Synpo2	**synaptopodin 2**	**3,25E-06**	**5,4934273**	**0**
Sh3bgr	SH3-binding domain glutamic acid-rich protein	1,75E-05	5,1266565	0
Txnip	thioredoxin interacting protein	0,003058237	4,9323688	0
Cnn1	**calponin 1**	**0,002651492**	**4,5607553**	**0**
Tgfb3	**transforming growth factor, beta 3**	**9,75E-05**	**4,479578**	**0**
Efhd1	EF hand domain containing 1	1,02E-08	4,219693	0
Nppb	natriuretic peptide type B	1,12E-06	4,0196276	0
Ifi27l2b	interferon, alpha-inducible protein 27 like 2B	3,60E-05	4,0013194	0
Tpm2	**tropomyosin 2, beta**	**5,55E-04**	**3,783665**	**0**
Casq2	**calsequestrin 2**	**0,002305424**	**3,663854**	**0**
Mmp17	matrix metallopeptidase 17	3,34E-05	3,5898006	0
Zim1	zinc finger, imprinted 1	0,00181821	3,44584	0
Susd5	sushi domain containing 5	5,04E-04	3,4297047	0
Xk	Kell blood group precursor (McLeod phenotype) homolog	4,04E-04	3,383706	0
Susd2	sushi domain containing 2	3,39E-05	3,3536263	0
Sost	sclerostin	4,21E-04	3,309478	0
Mcam	melanoma cell adhesion molecule	0,001033047	3,2800252	0
Svil	supervillin	3,88E-07	3,2691855	0
Mrvi1	MRV integration site 1	0,001209502	3,2522058	0
Slc16a4	solute carrier family 16, member 4	2,97E-04	3,247924	0
Atp8b1	ATPase, class I, type 8B, member 1	1,43E-05	3,2051013	0
Lmod1	**leiomodin 1 (smooth muscle)**	**4,17E-04**	**3,1801312**	**0**
Bves	**blood vessel epicardial substance**	**1,33E-05**	**3,1635838**	**0**
Wnt16	wingless-related MMTV integration site 16	0,001028933	3,161625	0
Itga5	**integrin alpha 5 (fibronectin receptor alpha)**	**2,76E-07**	**3,152299**	**0**
Atp2b4	ATPase, Ca++ transporting, plasma membrane 4	1,41E-05	3,114832	0
Popdc2	**popeye domain containing 2**	**1,20E-06**	**2,9238355**	**0**
Hspa1b	heat shock protein 1B	3,21E-05	2,828471	0
Mustn1	musculoskeletal, embryonic nuclear protein 1	3,49E-05	2,7880564	0
Ppp1r14a	protein phosphatase 1, regulatory (inhibitor) subunit 14A	0,001101076	2,78478	0
Diras2	DIRAS family, GTP-binding RAS-like 2	0,001340517	2,7329555	0
Adcy5	adenylate cyclase 5	1,00E-05	2,7325222	0
Myl9	**myosin, light polypeptide 9, regulatory**	**0,001506742**	**2,6924**	**0**
Tpm1	**tropomyosin 1, alpha**	**1,27E-04**	**2,684333**	**0**
Msrb1	methionine sulfoxide reductase B1	0,001009095	2,6795926	0
Scube3	signal peptide, CUB domain, EGF-like 3	4,95E-04	2,6530118	0
Nexn	nexilin	2,13E-04	2,6454408	0
Itga8	**integrin alpha 8**	**3,39E-04**	**2,629164**	**0**
Lcp1	lymphocyte cytosolic protein 1	0,002914813	2,6233037	0
Vcl	**vinculin**	**6,00E-04**	**2,6177256**	**0**
Haus8	4HAUS augmin-like complex, subunit 8	3,23E-05	2,6029716	0
Dtna	**dystrobrevin alpha**	**2,01E-07**	**2,5851405**	**0**
Npnt	nephronectin	5,07E-04	2,5170436	0
Itga1	**integrin alpha 1**	**4,97E-07**	**2,4899623**	**0**
Plau	plasminogen activator, urokinase	1,63E-04	2,4898348	0
Gcnt4	glucosaminyl (N-acetyl) transferase 4, core 2	0,002039047	2,472116	0
Hspb1	heat shock protein 1	5,88E-05	2,4475944	0

Table 2

	No diabetes	Type 2 diabetes	P value
Systolic blood pressure (mmHg)	132.5±9.0	147.5±11.6	P = 0.33
Diastolic blood pressure (mmHg)	75.8±5.1	83±6.5	P = 0.39
Blood glucose (mM)	6.3±0.4	10.1±0.4	***P<0.001
LDL cholesterol (mM)	2.8±0.6	2.8±0.3	P = 0.93
Serum creatinine (μM)	87.3±4.9	96±18	P = 0.59

Table 1

Gene Symbol	Gene Description	T-test(p-value)	Fold Change	q-value (%)
Acta1	**actin, alpha 1, skeletal muscle**	**7,63E-08**	**8,596519**	**0**
Myh11	**myosin, heavy polypeptide 11, smooth muscle**	**3,64E-05**	**8,130582**	**0**
Actg2	**actin, gamma 2, smooth muscle, enteric**	**4,13E-04**	**6,7903028**	**0**
Synpo2	**synaptopodin 2**	**3,25E-06**	**5,4934273**	**0**
Sh3bgr	SH3-binding domain glutamic acid-rich protein	1,75E-05	5,1266565	0
Txnip	thioredoxin interacting protein	0,003058237	4,9323688	0
Cnn1	**calponin 1**	**0,002651492**	**4,5607553**	**0**
Tgfb3	**transforming growth factor, beta 3**	**9,75E-05**	**4,479578**	**0**
Efhd1	EF hand domain containing 1	1,02E-08	4,219693	0
Nppb	natriuretic peptide type B	1,12E-06	4,0196276	0
Ifi27l2b	interferon, alpha-inducible protein 27 like 2B	3,60E-05	4,0013194	0
Tpm2	**tropomyosin 2, beta**	**5,55E-04**	**3,783665**	**0**
Casq2	**calsequestrin 2**	**0,002305424**	**3,663854**	**0**
Mmp17	matrix metallopeptidase 17	3,34E-05	3,5898006	0
Zim1	zinc finger, imprinted 1	0,00181821	3,44584	0
Susd5	sushi domain containing 5	5,04E-04	3,4297047	0
Xk	Kell blood group precursor (McLeod phenotype) homolog	4,04E-04	3,383706	0
Susd2	sushi domain containing 2	3,39E-05	3,3536263	0
Sost	sclerostin	4,21E-04	3,309478	0
Mcam	melanoma cell adhesion molecule	0,001033047	3,2800252	0
Svil	supervillin	3,88E-07	3,2691855	0
Mrvi1	MRV integration site 1	0,001209502	3,2522058	0
Slc16a4	solute carrier family 16, member 4	2,97E-04	3,247924	0
Atp8b1	ATPase, class I, type 8B, member 1	1,43E-05	3,2051013	0
Lmod1	**leiomodin 1 (smooth muscle)**	**4,17E-04**	**3,1801312**	**0**
Bves	**blood vessel epicardial substance**	**1,33E-05**	**3,1635838**	**0**
Wnt16	wingless-related MMTV integration site 16	0,001028933	3,161625	0
Itga5	**integrin alpha 5 (fibronectin receptor alpha)**	**2,76E-07**	**3,152299**	**0**
Atp2b4	ATPase, Ca++ transporting, plasma membrane 4	1,41E-05	3,114832	0
Popdc2	**popeye domain containing 2**	**1,20E-06**	**2,9238355**	**0**
Hspa1b	heat shock protein 1B	3,21E-05	2,828471	0
Mustn1	musculoskeletal, embryonic nuclear protein 1	3,49E-05	2,7880564	0
Ppp1r14a	protein phosphatase 1, regulatory (inhibitor) subunit 14A	0,001101076	2,78478	0
Diras2	DIRAS family, GTP-binding RAS-like 2	0,001340517	2,7329555	0
Adcy5	adenylate cyclase 5	1,00E-05	2,7325222	0
Myl9	**myosin, light polypeptide 9, regulatory**	**0,001506742**	**2,6924**	**0**
Tpm1	**tropomyosin 1, alpha**	**1,27E-04**	**2,684333**	**0**
Msrb1	methionine sulfoxide reductase B1	0,001009095	2,6795926	0
Scube3	signal peptide, CUB domain, EGF-like 3	4,95E-04	2,6530118	0
Nexn	nexilin	2,13E-04	2,6454408	0
Itga8	**integrin alpha 8**	**3,39E-04**	**2,629164**	**0**
Lcp1	lymphocyte cytosolic protein 1	0,002914813	2,6233037	0
Vcl	**vinculin**	**6,00E-04**	**2,6177256**	**0**
Haus8	4HAUS augmin-like complex, subunit 8	3,23E-05	2,6029716	0
Dtna	**dystrobrevin alpha**	**2,01E-07**	**2,5851405**	**0**
Npnt	nephronectin	5,07E-04	2,5170436	0
Itga1	**integrin alpha 1**	**4,97E-07**	**2,4899623**	**0**
Plau	plasminogen activator, urokinase	1,63E-04	2,4898348	0
Gcnt4	glucosaminyl (N-acetyl) transferase 4, core 2	0,002039047	2,472116	0
Hspb1	heat shock protein 1	5,88E-05	2,4475944	0

Table 2

	No diabetes	Type 2 diabetes	P value
Systolic blood pressure (mmHg)	132.5±9.0	147.5±11.6	P = 0.33
Diastolic blood pressure (mmHg)	75.8±5.1	83±6.5	P = 0.39
Blood glucose (mM)	6.3±0.4	10.1±0.4	***P<0.001
LDL cholesterol (mM)	2.8±0.6	2.8±0.3	P = 0.93
Serum creatinine (μM)	87.3±4.9	96±18	P = 0.59

Figure 1

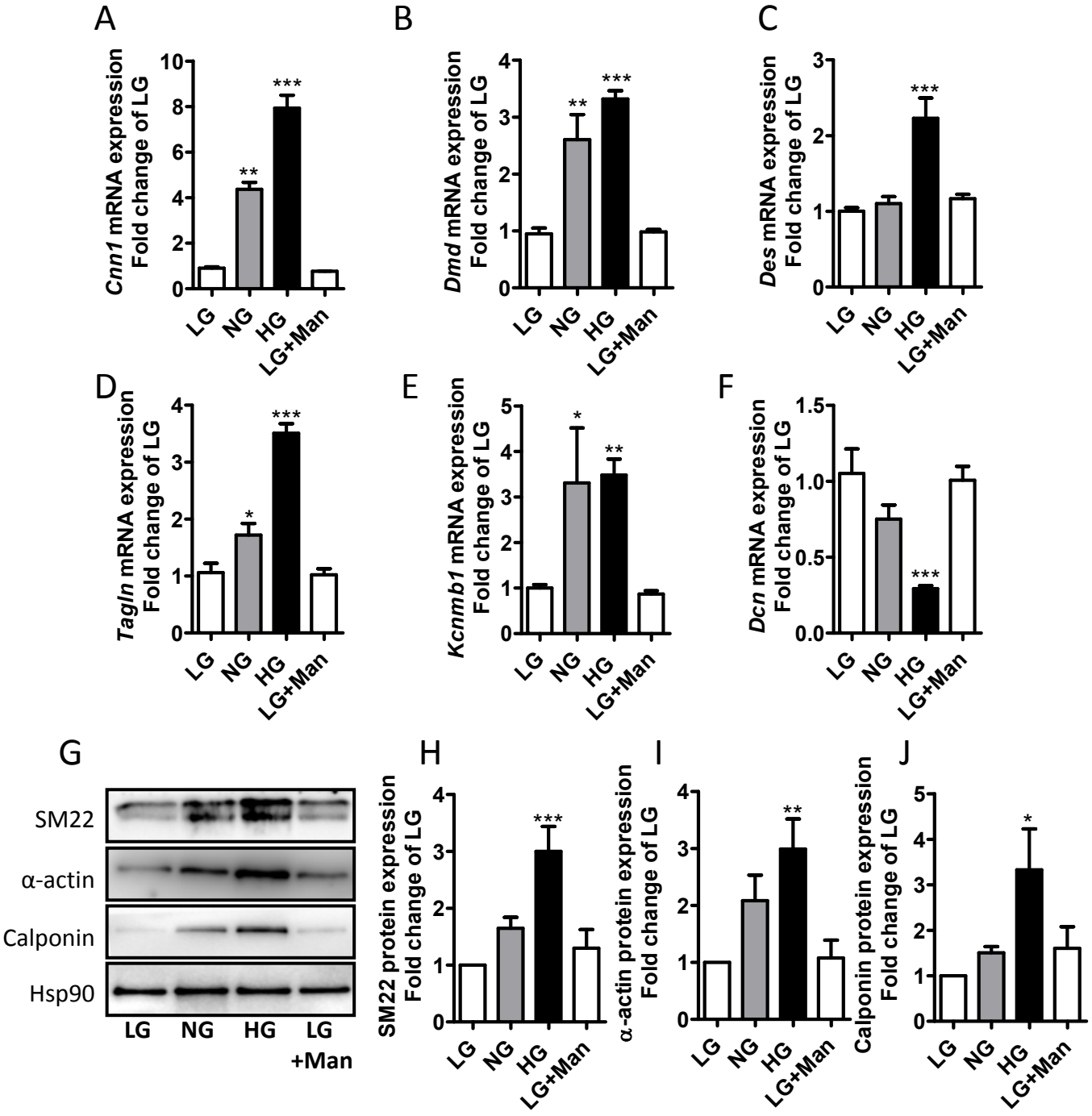
A
Cnn1 mRNA expression
Fold change of LG
B
Dmd mRNA expression
Fold change of LG
C
Des mRNA expression
Fold change of LG
D
Tagln mRNA expression
Fold change of LG
E
Kcnmb1 mRNA expression
Fold change of LG
F
Dcn mRNA expression
Fold change of LG
LG
NG
HG
LG+Man
G
SM22
α-actin
Calponin
Hsp90
LG
NG
HG
LG
+Man
H
SM22 protein expression
Fold change of LG
I
α-actin protein expression
Fold change of LG
J
Calponin protein expression
Fold change of LG

Figure 2

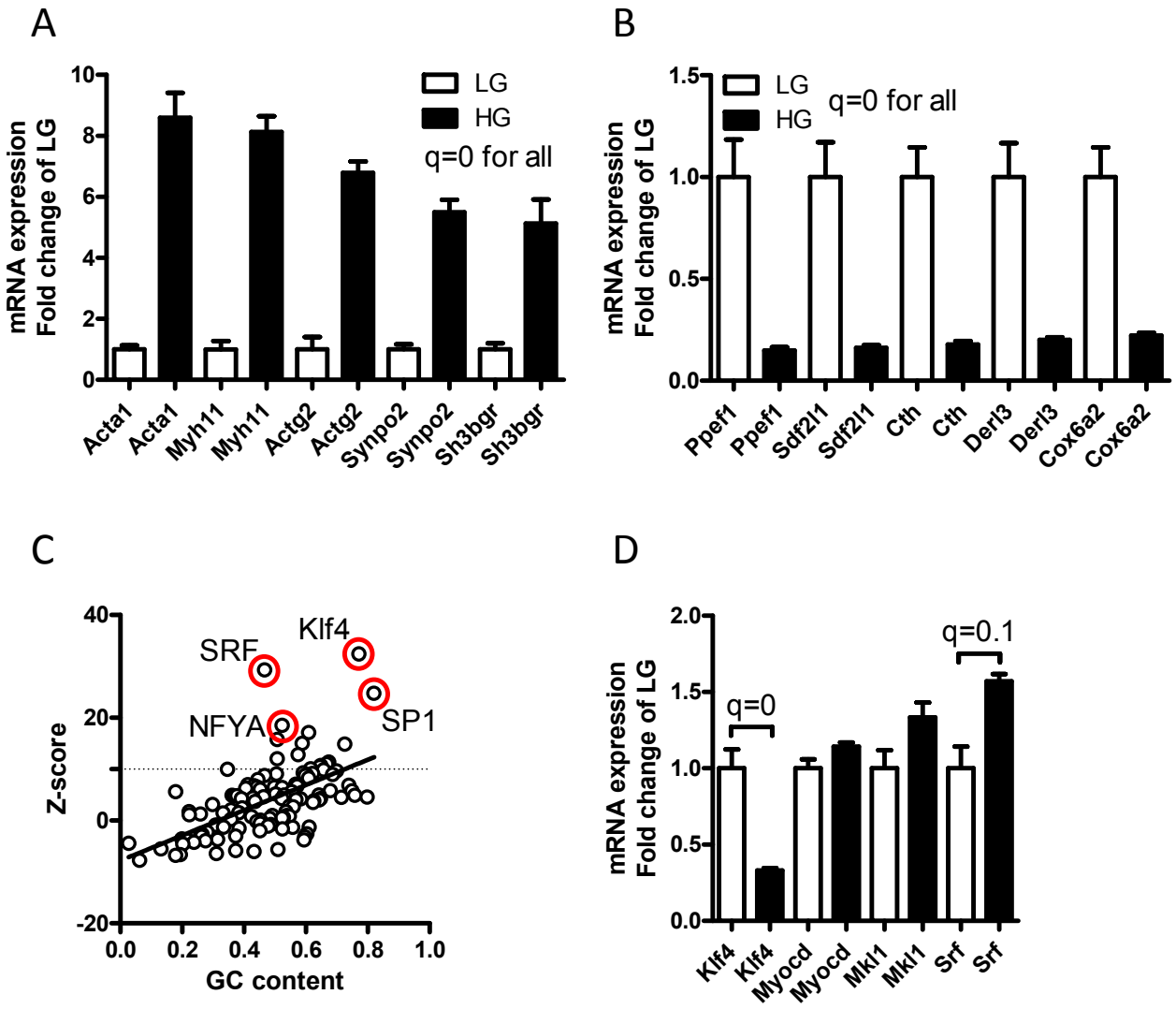
A
mRNA expression
Fold change of LG
LG
HG
q=0 for all
Acta1
Acta1
Myh11
Myh11
Actg2
Actg2
Synpo2
Synpo2
Sh3bgr
Sh3bgr
B
mRNA expression
Fold change of LG
LG
HG
q=0 for all
Ppef1
Ppef1
Sdf2l1
Sdf2l1
Cth
Cth
Derl3
Derl3
Cox6a2
Cox6a2
C
Z-score
GC content
SRF
Klf4
NFYA
SP1
D
mRNA expression
Fold change of LG
q=0
q=0.1
Klf4
Klf4
Myocd
Myocd
Mkl1
Mkl1
Srf
Srf

Figure 3

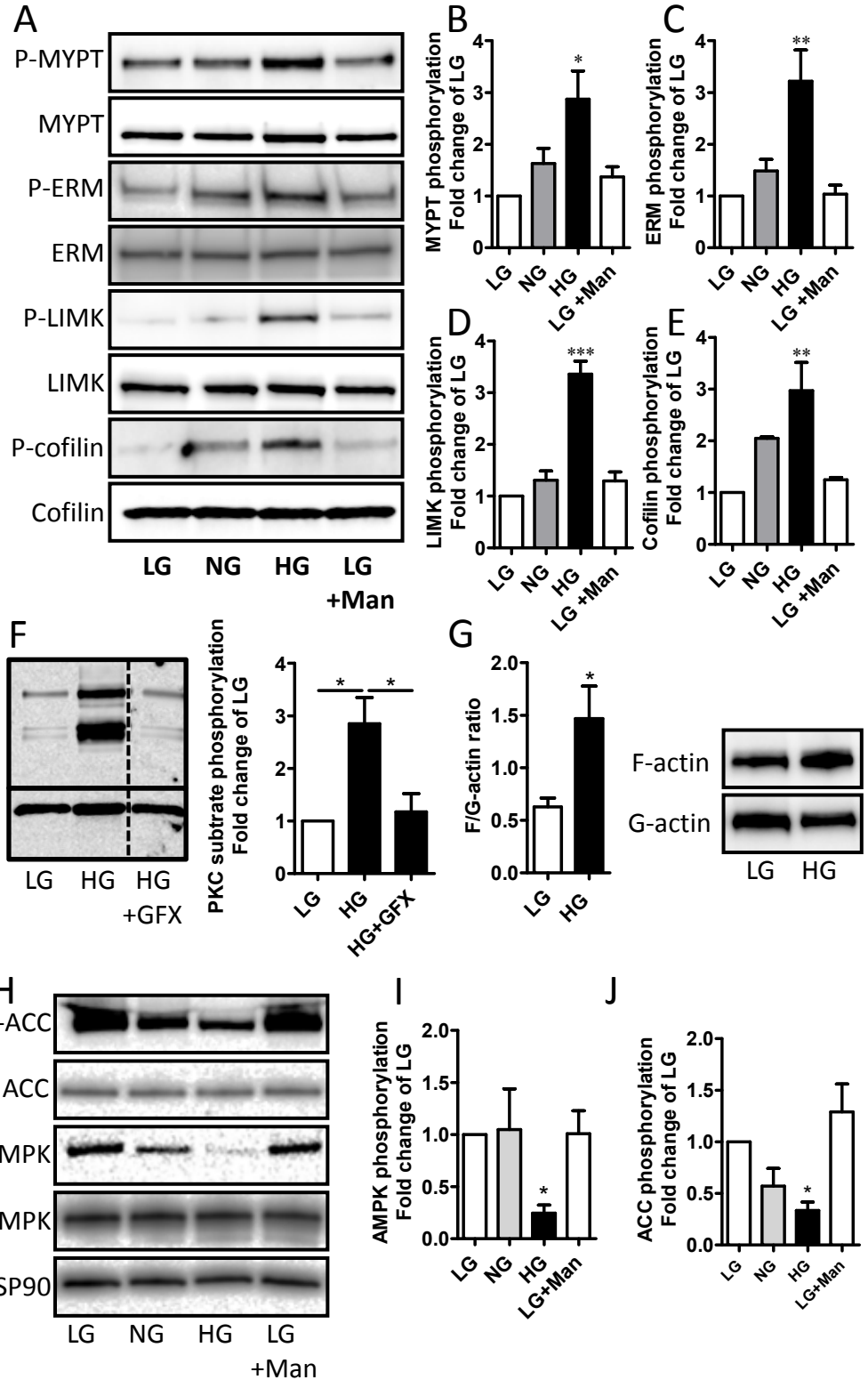
A
P-MYPT
MYPT
P-ERM
ERM
P-LIMK
LIMK
P-cofilin
Cofilin
LG
NG
HG
LG +Man
B
MYPT phosphorylation Fold change of LG
C
ERM phosphorylation Fold change of LG
D
LIMK phosphorylation Fold change of LG
E
Cofilin phosphorylation Fold change of LG
F
LG
HG
HG +GFX
PKC subtrate phosphorylation Fold change of LG
HG+GFX
G
F/G-actin ratio
F-actin
G-actin
H
P-ACC
ACC
P-AMPK
AMPK
HSP90
I
AMPK phosphorylation Fold change of LG
J
ACC phosphorylation Fold change of LG

Figure 4

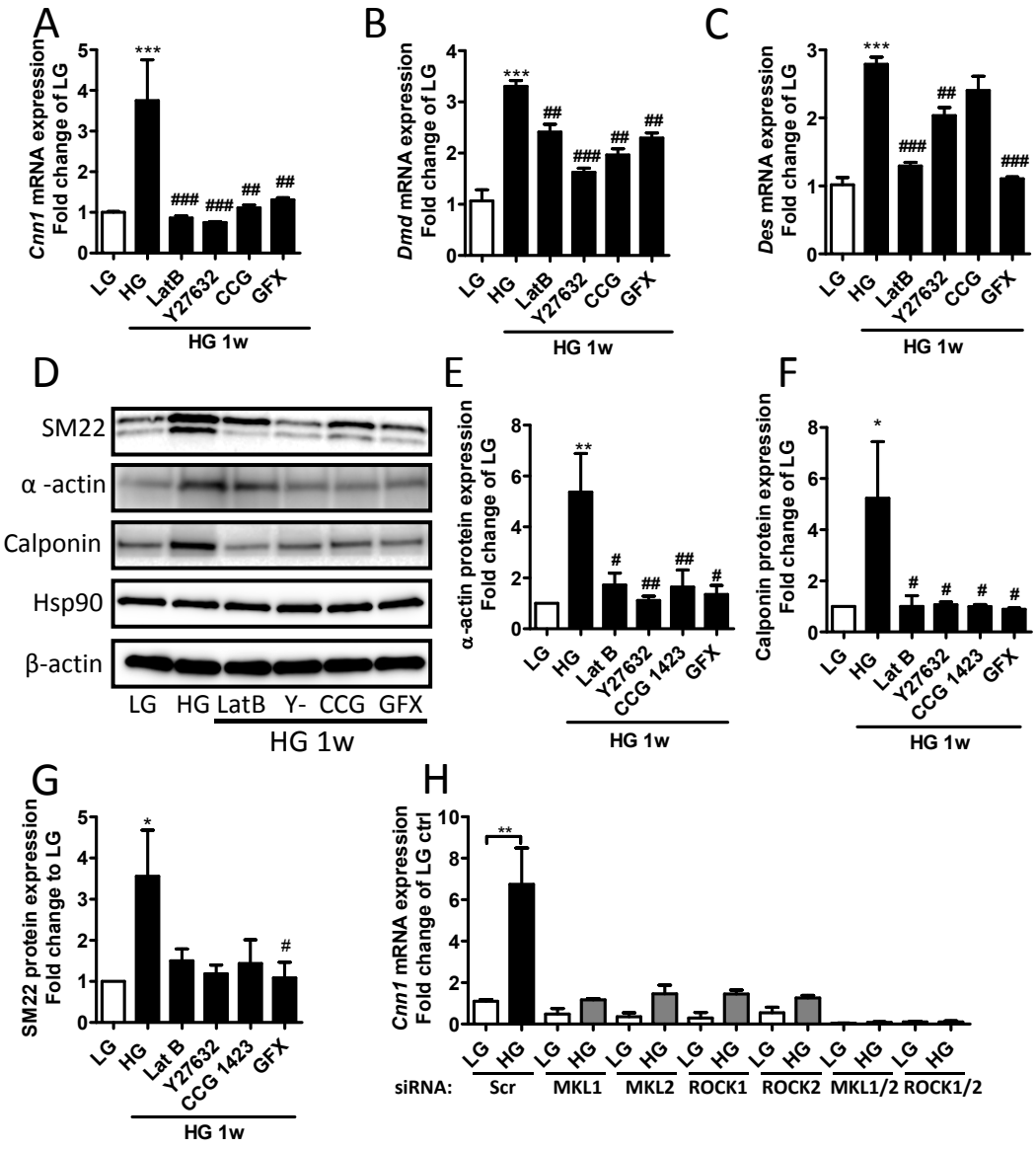
A
Cnn1 mRNA expression
Fold change of LG
LG
HG
LatB
Y27632
CCG
GFX
HG 1w
B
Dmd mRNA expression
Fold change of LG
C
Des mRNA expression
Fold change of LG
D
SM22
α -actin
Calponin
Hsp90
β-actin
LG HG LatB Y- CCG GFX
HG 1w
E
α-actin protein expression
Fold change of LG
Lat B
CCG 1423
F
Calponin protein expression
Fold change of LG
G
SM22 protein expression
Fold change to LG
H
Cnn1 mRNA expression
Fold change of LG ctrl
siRNA:
Scr
MKL1
MKL2
ROCK1
ROCK2
MKL1/2
ROCK1/2

Figure 5

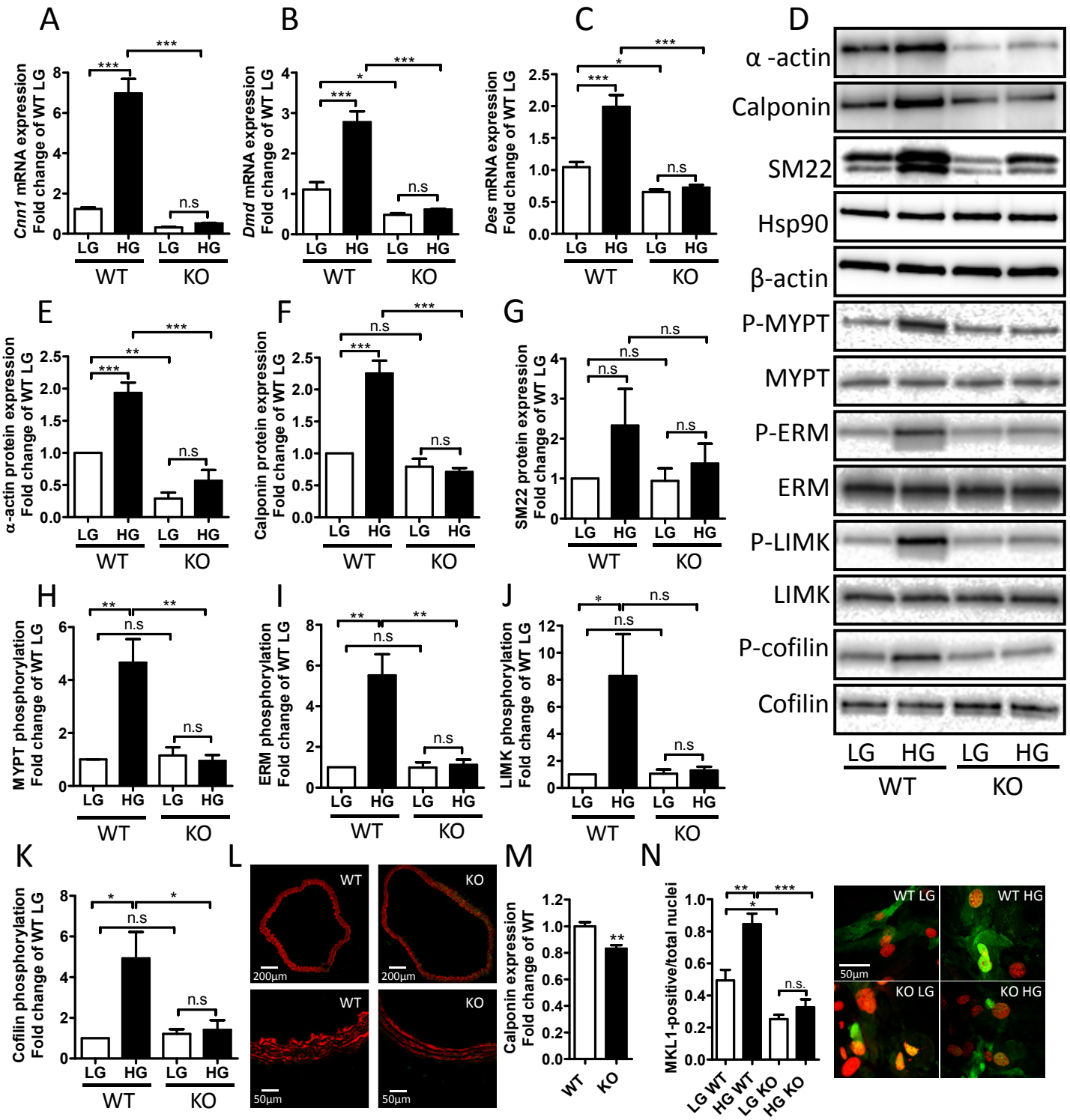
A
Cnn1 mRNA expression Fold change of WT LG
B
Dmd mRNA expression Fold change of WT LG
C
Des mRNA expression Fold change of WT LG
D
α -actin
Calponin
SM22
Hsp90
β-actin
P-MYPT
MYPT
P-ERM
ERM
P-LIMK
LIMK
P-cofilin
Cofilin
LG HG LG HG
WT KO
E
α-actin protein expression Fold change of WT LG
F
Calponin protein expression Fold change of WT LG
G
SM22 protein expression Fold change of WT LG
H
MYPT phosphorylation Fold change of WT LG
I
ERM phosphorylation Fold change of WT LG
J
LIMK phosphorylation Fold change of WT LG
K
Cofilin phosphorylation Fold change of WT LG
L
WT
KO
200μm
50μm
M
Calponin expression Fold change of WT
WT KO
N
MKL1-positive/total nuclei
LG WT HG WT LG KO HG KO
WT LG
WT HG
KO LG
KO HG
50μm
n.s
n.s.

Figure 6

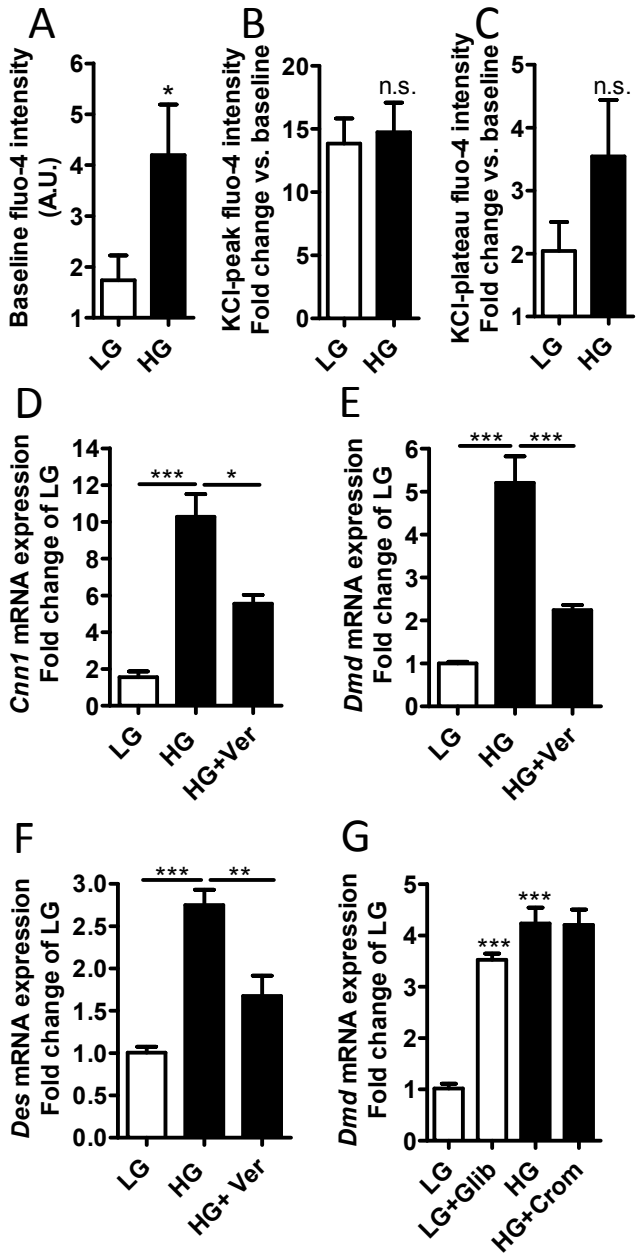
A
Baseline fluo-4 intensity (A.U.)
*
LG
HG
B
KCl-peak fluo-4 intensity Fold change vs. baseline
n.s.
LG
HG
C
KCl-plateau fluo-4 intensity Fold change vs. baseline
n.s.
LG
HG
D
Cnn1 mRNA expression Fold change of LG
***
*
LG
HG
HG+Ver
E
Dmd mRNA expression Fold change of LG
***
***
LG
HG
HG+Ver
F
Des mRNA expression Fold change of LG
***
**
LG
HG
HG+ Ver
G
Dmd mRNA expression Fold change of LG
***
***
LG
LG+Glib
HG
HG+Crom

Figure 7

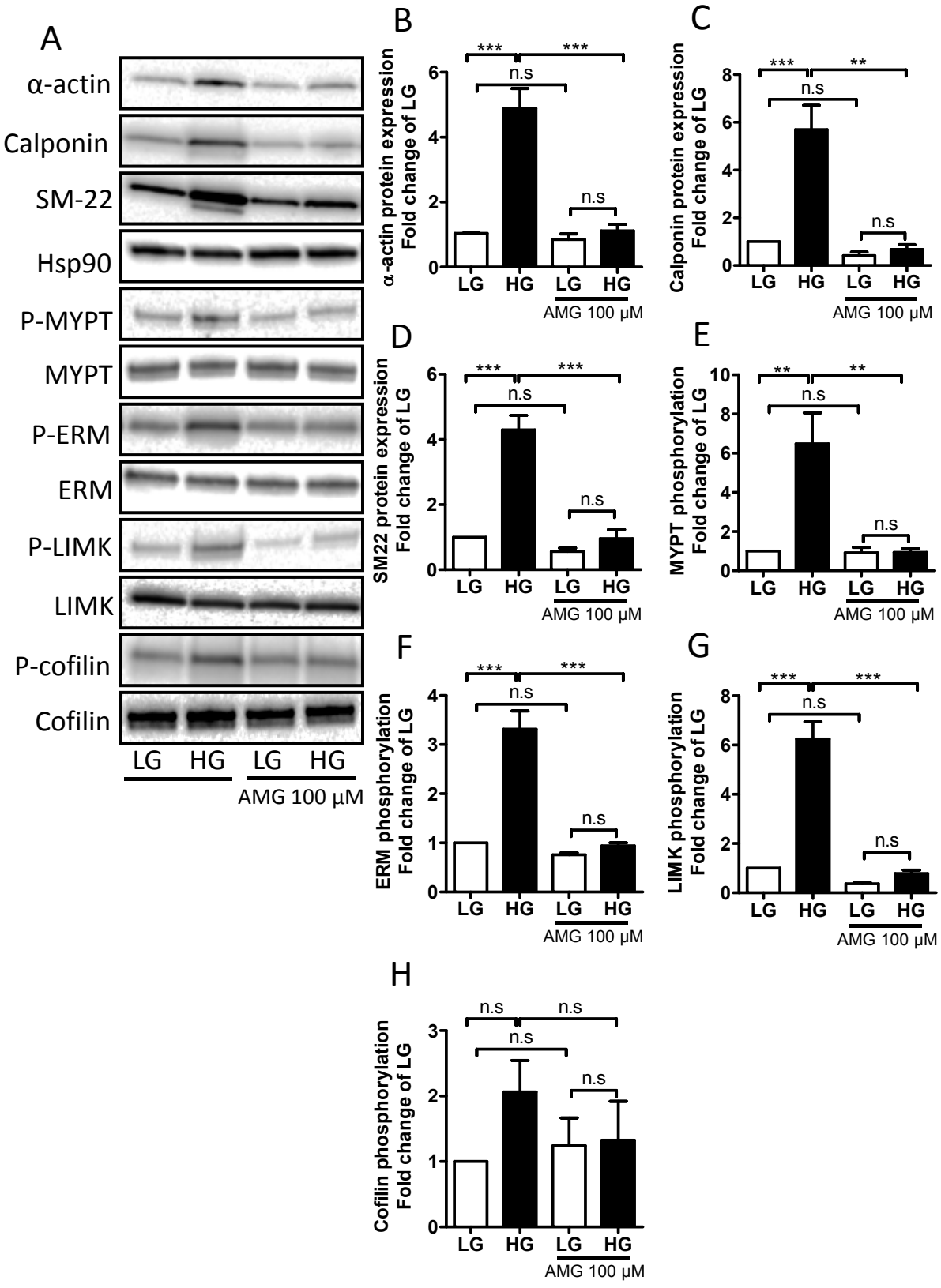
A
α-actin
Calponin
SM-22
Hsp90
P-MYPT
MYPT
P-ERM
ERM
P-LIMK
LIMK
P-cofilin
Cofilin
LG HG LG HG
AMG 100 μM
B
α-actin protein expression Fold change of LG
C
Calponin protein expression Fold change of LG
D
SM22 protein expression Fold change of LG
E
MYPT phosphorylation Fold change of LG
F
ERM phosphorylation Fold change of LG
G
LIMK phosphorylation Fold change of LG
H
Cofilin phosphorylation Fold change of LG
***
**
n.s
LG HG LG HG
AMG 100 μM

Figure 8

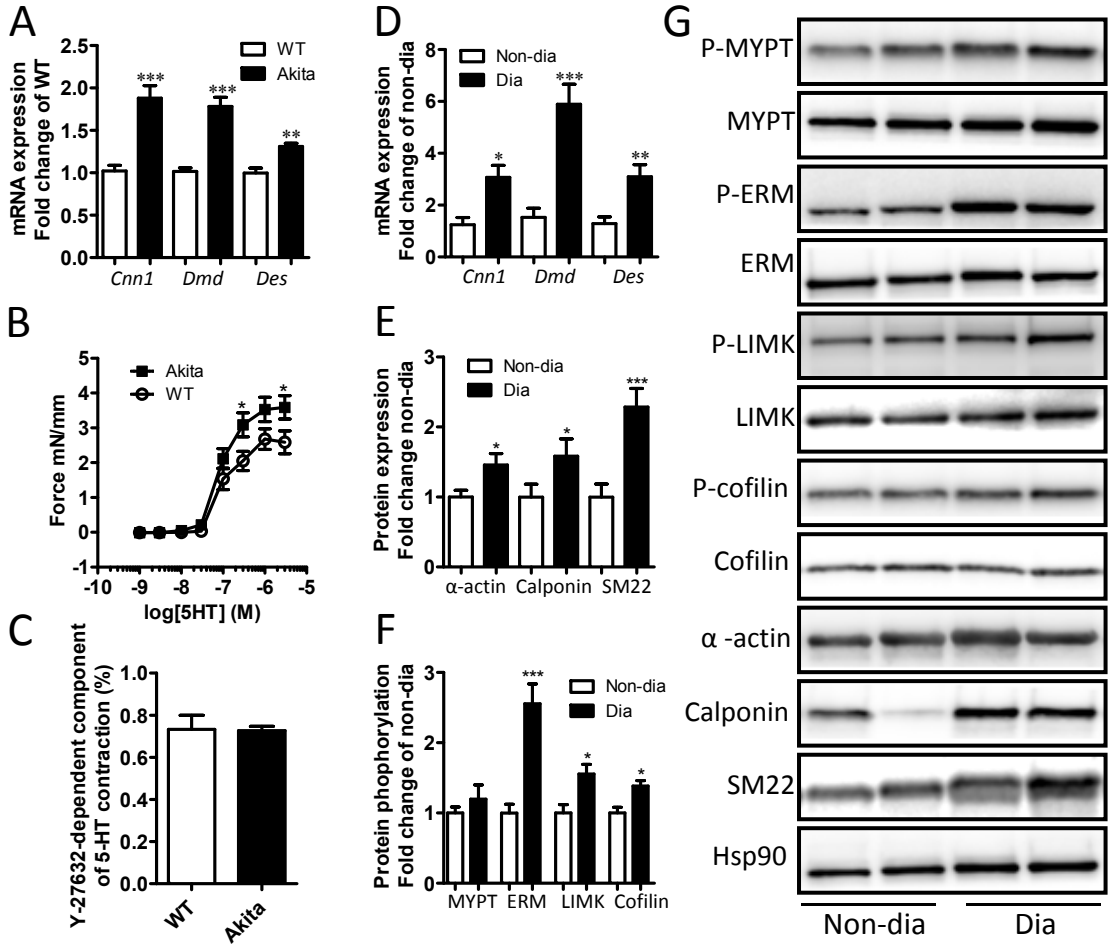
A
mRNA expression
Fold change of WT
WT
Akita
Cnn1
Dmd
Des
B
Force mN/mm
Akita
WT
log[5HT] (M)
C
Y-27632-dependent component
of 5-HT contraction (%)
WT
Akita
D
mRNA expression
Fold change of non-dia
Non-dia
Dia
Cnn1
Dmd
Des
E
Protein expression
Fold change non-dia
Non-dia
Dia
α-actin
Calponin
SM22
F
Protein phophorylation
Fold change of non-dia
Non-dia
Dia
MYPT
ERM
LIMK
Cofilin
G
P-MYPT
MYPT
P-ERM
ERM
P-LIMK
LIMK
P-cofilin
Cofilin
α -actin
Calponin
SM22
Hsp90
Non-dia
Dia